

Review

A Review of Equivalent Circuit Model Based Online State of Power Estimation for Lithium-Ion Batteries in Electric Vehicles

Ruohan Guo and Weixiang Shen * 

School of Science, Computing and Engineering Technologies, Swinburne University of Technology, Hawthorn, VA 3122, Australia; rguo@swin.edu.au

* Correspondence: wshen@swin.edu.au

Abstract: With rapid transportation electrification worldwide, lithium-ion batteries have gained much attention for energy storage in electric vehicles (EVs). State of power (SOP) is one of the key states of lithium-ion batteries for EVs to optimise power flow, thereby requiring accurate online estimation. Equivalent circuit model (ECM)-based methods are considered as the mainstream technique for online SOP estimation. They primarily vary in their basic principle, technical contribution, and validation approach, which have not been systematically reviewed. This paper provides an overview of the improvements on ECM-based online SOP estimation methods in the past decade. Firstly, online SOP estimation methods are briefed, in terms of different operation modes, and their main pros and cons are also analysed accordingly. Secondly, technical contributions are reviewed from three aspects: battery modelling, online parameters identification, and SOP estimation. Thirdly, SOP testing methods are discussed, according to their accuracy and efficiency. Finally, the challenges and outlooks are presented to inspire researchers in this field for further developments in the future.

Keywords: online state of power estimation; equivalent-circuit model; lithium-ion battery; electrical vehicle; review



Citation: Guo, R.; Shen, W. A Review of Equivalent Circuit Model Based Online State of Power Estimation for Lithium-Ion Batteries in Electric Vehicles. *Vehicles* **2022**, *4*, 1–29. <https://doi.org/10.3390/vehicles4010001>

Academic Editors: Chen Lv and Xiaosong Hu

Received: 26 October 2021

Accepted: 17 December 2021

Published: 21 December 2021

Publisher's Note: MDPI stays neutral with regard to jurisdictional claims in published maps and institutional affiliations.



Copyright: © 2021 by the authors. Licensee MDPI, Basel, Switzerland. This article is an open access article distributed under the terms and conditions of the Creative Commons Attribution (CC BY) license (<https://creativecommons.org/licenses/by/4.0/>).

1. Introduction

Transportation electrification, such as electric vehicles (EVs), is a clean solution to the replacement of traditional internal combustion engine vehicles for tailpipe emissions reduction [1]. In recent years, lithium-ion batteries, as energy storage in EVs, have gained much popularity in industry and academia, owing to their high specific energy and power density, long service life, and light weight [2–4]. However, they are inclined to suffer from potential safety issues during service, such as internal short circuit and thermal runaway. To ensure the safety and durability of lithium-ion batteries in EV applications, battery management systems (BMSs) are equipped to monitor battery states [5]. State of power (SOP), as one of the key states of lithium ion batteries, plays a pivotal role in optimising energy efficiency and choosing EV driving strategy during acceleration, regenerative braking, and gradient climbing [6,7]. Since SOP is a non-measurable battery state, with strong time-variability, it is of great importance to devise an effective and efficient method to achieve online SOP estimation in BMSs for EVs. However, SOP has a coupling effect with other battery states, including state of charge (SOC), state of energy (SOE), state of temperature (SOT), and state of health (SOH), thereby making accurate online SOP estimation more difficult in practice. Among them, SOC and SOE correspond to battery open-circuit voltage (OCV) and, thus, relate to the usable voltage range for SOP estimation in a prediction window, while SOT and SOH affect battery internal resistance and the relationship between OCV and SOC (SOE) and, thus, have strong influence on SOP. Although online SOP estimation has been extensively researched, challenges are still faced in different aspects [8].

To date, SOP estimation techniques mainly fall into two groups: characteristic mapping (CM)-based methods and equivalent circuit model (ECM)-based methods [9]. The

first group make use of the identified interdependences between battery parameters and battery power characteristics to implement online feature mapping of SOP. However, they cannot reproduce battery internal dynamics, require a large storage capacity from BMSs, and lack robustness over battery lifetime, all of which become a major obstacle in EV applications. Compared with the CM-based methods, ECM-based online SOP estimation methods have been the mainstream technique, due to their accurate description of battery internal dynamics, strong robustness and adaptability, relatively low computational cost, and satisfactory estimation performance. Plett first applied a lumped ECM to describe OCV variation for online SOP estimation [10]. Then, a variety of improved ECM-based online SOP estimation methods have emerged in the past decade, and it is necessary to systematically review and compare these methods and recognise their improvements.

The remainder of this paper is organized as follows: Section 2 introduces basic principles of online SOP estimation, in terms of different operation modes. Section 3 explains the technical improvements and contributions in the past decade from three perspectives: battery modelling, model parameters identification, and SOP estimation. Section 4 summarizes SOP calibration methods, based on their accuracies and efficiencies. Challenges and outlooks are presented in Section 5. Finally, conclusions are drawn in Section 6.

2. Online SOP Estimation

In this paper, SOP is defined as the peak power capability that a battery could deliver or receive over a prediction window while keeping the battery within the safe operating area [9]. According to this definition, online SOP estimation can be generally carried out at three operation modes, namely constant current (CC), constant voltage (CV) and constant current constant voltage (CCCV) modes. Thus, different open-loop prediction methods (OLPMs) for online SOP estimation are derived accordingly.

2.1. SOP Estimation at a Constant Current Mode

In the OLPM for online SOP estimation at a CC mode, a battery is supposed to continuously operate at constant current throughout a prediction window [11]. Assume the prediction window (ranging from time k to $k + L$), battery current, and terminal voltage during this period can be depicted in Figure 1, where discharge current is assumed to be positive, while charge current is negative.

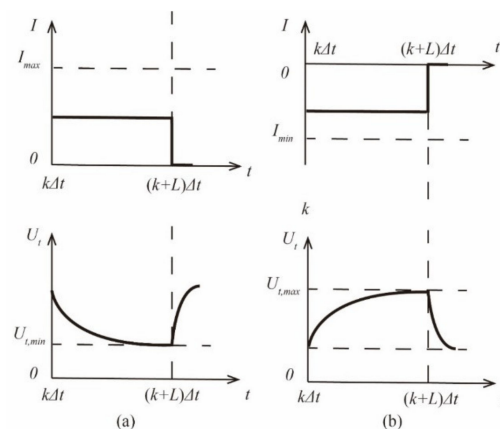


Figure 1. Battery current and terminal voltage in SOP estimation at a constant current mode: (a) discharge; (b) charge.

It can be seen that the terminal voltage of a battery will monotonically decline (or grow) in the CC discharge (or charge) mode. Therefore, SOP depends on the power capability at the end-of-window. Comparing with other constraints (e.g., current limit and SOC limit), voltage limit is a major concern in the CC mode, which requires accurately predicting battery terminal voltage at the end of a prediction window, based on the employed ECM.

Battery SOP is determined once battery terminal voltage reaches its lower (or upper) cut-off value, namely $U_{t,k+L} = U_{t,\min}$ (or $U_{t,\max}$) [12].

2.2. SOP Estimation at a Constant Voltage Mode

In the OLPM for online SOP estimation at a CV mode, a battery is forced to continuously operate at its lower (or upper) cut-off voltage throughout a prediction window [13]. As depicted in Figure 2, the peak discharge current would monotonically decrease, while the peak charge current exhibits an opposite trend in this period. Therefore, accurately capturing the current variation trend is required, based on the employed ECM during the prediction window, while the battery terminal voltage is deemed to be kept at $U_{t,\min}$ (or $U_{t,\max}$).

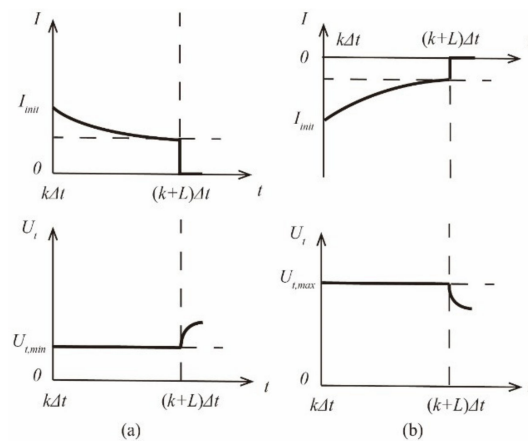


Figure 2. Battery current and terminal voltage in SOP estimation at a constant voltage mode: (a) discharge; (b) charge.

2.3. SOP Estimation at a Constant Current Constant Voltage Mode

In the OLPM for online SOP estimation at a CCCV mode, a battery is operating at current limit at a CC mode at the very beginning and will shift from the CC mode to the CV mode once battery terminal voltage reaches voltage limit, as depicted in Figure 3 [14]. It can be observed that pinpointing the timing shift from the CC mode to the CV mode is the key to work out the peak power of the CCCV mode. Such a critical timing occurs when a battery is operating at its pre-set current limit, while its terminal voltage reaches $U_{t,\min}$ (or $U_{t,\max}$). Afterwards, the battery will turn to the CV mode, and the load current has to reduce to avoid breaking the pre-set voltage limit.

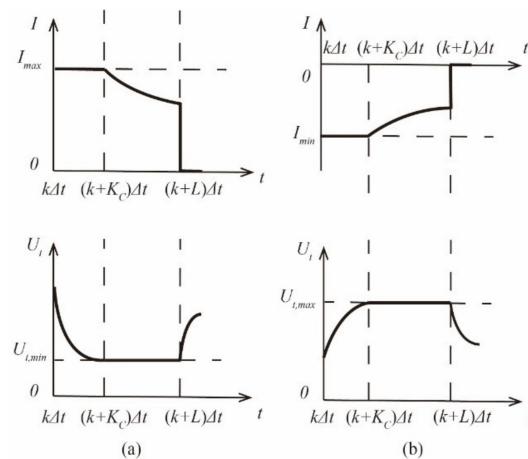


Figure 3. Battery current and terminal voltage in SOP estimation at a constant current constant voltage mode: (a) discharge; (b) charge.

From the OLPMs for online SOP estimation at CC, CV, and CCCV modes, introduced above, their correlation and corresponding pros and cons are analysed in the following:

1. The OLPMs at CC and CV modes keep a battery operating within a safe voltage range by reducing either peak average current or peak instantaneous current in a prediction window, which are more straightforward than the OLPM at a CCCV mode. It is worth noting that the OLPMs at the CC and CV modes are essentially the same when the length of the prediction window L is taken as one.
2. The OLPM at a CV mode does not take current limit into account. This may cause an over-optimistic SOP estimation at high (or low) SOC regions during the discharge (or charge) process. To involve current limit, the OLPM at a CCCV mode is developed.
3. The OLPM at a CC mode provides a relatively conservative, yet stable, peak current estimation, which is of benefit to the development of a long-term (>30 s) driving strategy for EVs. By contrast, OLPMs at CV and CCCV modes are more suitable for a short term (<10 s) driving strategy for EVs. However, they may provide an over-aggressive driving strategy by ideally assuming a constant OCV in a lengthy prediction window, while making the best use of battery voltage range to supply as much power as possible at every instant. In consequence, EVs may acquire a strong power supply in a short period but fall into energy poverty very soon, since the battery OCV would gradually decline, and the real peak current is going to drop more rapidly than expected after a battery being shifted to a CV mode.
4. The OLPMs at CV and CCCV modes may risk batteries in overcharging and over-discharging, since they require fairly accurate knowledge about SOC and battery model in real-time to perfectly hold a battery at voltage limit throughout a prediction window.

3. Improvements on ECM-Based Method for Online SOP Estimation

3.1. Improvements on Battery Modelling

3.1.1. Improved 1-RC Model

To date, a variety of well-performed ECMs, with complex model structure, are proposed to capture battery electrochemical processes in great detail for battery state estimation. Relevant reviews can be found in [15–18]. Nevertheless, 1-RC model, as shown in Figure 4, is still the first choice for online SOP estimation, mainly because of its simplicity and ease of implementation. However, two apparent shortages limit its performance in real applications. (1) Structure imperfections: basic 1-RC model is unable to accurately reproduce some specific reactions and nonlinearities of lithium-ion batteries (e.g., hysteresis effect and diffusion process); (2) Parameters variability: model parameters of 1-RC model are in relation to various intrinsic and extrinsic factors (e.g., SOC, current, and temperature). Neglecting these dependencies would affect model accuracy under varying battery states and changeable operating conditions. Thus, efforts have been made on these two aspects to facilitate its competitiveness in online SOP estimation.

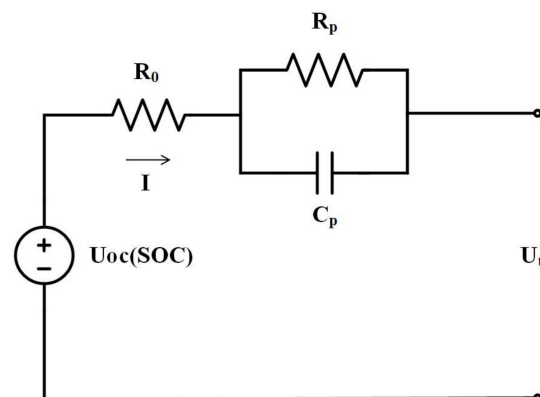


Figure 4. 1-RC model.

In pursuit of a more accurate battery model in SOP estimation, some specially designed components are introduced into a basic 1-RC model to reflect battery diffusion phenomenon, hysteresis effect, and self-discharge process.

In [19], a 1-RC model with diffusion resistance, as shown in Figure 5, is constructed to mimic battery diffusion phenomenon in a low frequency region for long-term SOP estimation. The time-dependent diffusion resistance is characterised based on a mass of experimental data. As an advantage, the alteration of the model structure will not influence the derivation of peak discharge and charge current. The experimental results show that the proposed model could effectively improve the SOP estimation accuracy in a prediction window over 10 s. However, the adaptability and robustness of the empirically-derived diffusion resistance needs to be further examined under different driving scenarios.

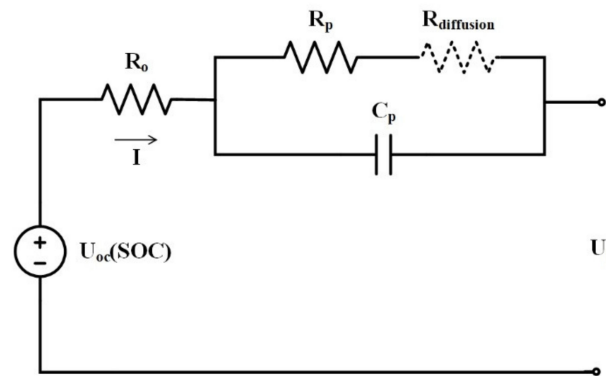


Figure 5. 1-RC model with diffusion resistance [19].

In [20–23], a 1-RC model with one-state hysteresis, as shown in Figure 6, is employed to capture battery hysteresis effect between battery charge and discharge trajectories. The peak power characteristics of LiFePO4 batteries are investigated under different operating conditions in [20]. According to the authors, the absence of hysteresis dynamics in basic 1-RC models will significantly affect SOP estimation of LiFePO4 batteries. Referring to [16], from the same authors, 1-RC model with one-state hysteresis is found as the best choice for LiFePO4 batteries, amid 12 commonly used ECMs, which offsets a notable voltage hysteresis and alleviates the model error by 7.9%, compared to basic 1-RC model. However, a main challenge of this model for online SOP estimation lies in that it is unable to directly formulate an analytical expression of peak discharge and charge current, due to the high nonlinearity of the current-dependent hysteresis voltage. Consequently, a numerical method, such as the bisection and Levenberg–Marquardt algorithms, is often resorted to, in order to solve the peak currents from a strong nonlinear equation.

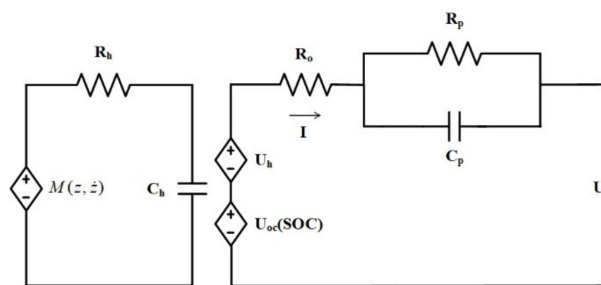


Figure 6. 1-RC model with one-state hysteresis [20–23].

In [24], a joint estimation algorithm of both SOC and SOP is proposed, based on a 1-RC model considering the self-discharge phenomenon. As shown in Figure 7, a runtime-based model (in the left part) comprises of a capacity, self-discharge resistance, and controlled current source in parallel, aiming to simulate the effects of battery cycling and calendar aging on available battery capacity in the long run.

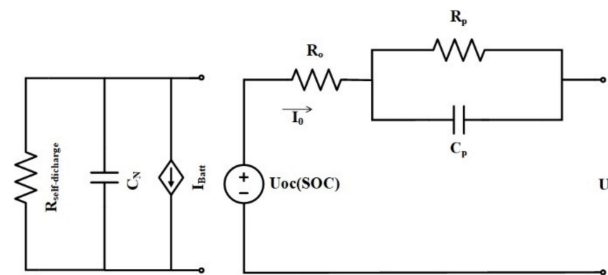


Figure 7. 1-RC model considering self-discharge phenomenon [24].

In [25], the authors state that the model error of a basic 1-RC model can result from a broad-frequency band. In view of this, a 1-RC model with a moving average noise, as shown in Figure 8, is proposed.

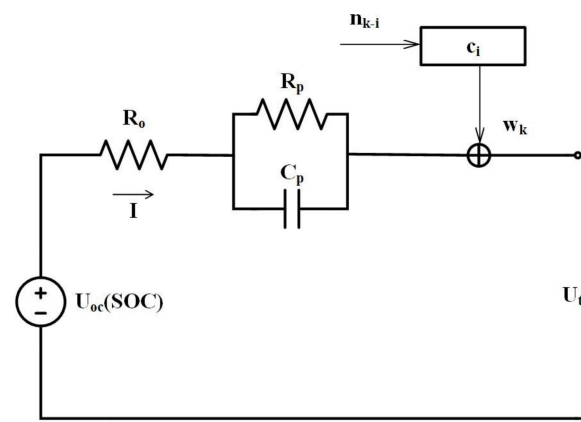


Figure 8. 1-RC model with a moving average noise [25].

Since Gaussian white noise covers a whole frequency range, the proposed model takes advantages of this nature to emulate the model error through a linear combination of a sequential Gaussian white noise in a moving average window. After being transformed to a linear regression form, the weight vector of the moving average model can be online regressed, together with other model parameters, to realise adaptability, which contributes to the precision of SOP estimation. Compared with basic 1-RC model, the 1-RC model with a moving average noise could strikingly reduce the voltage error under various load profiles.

Other than the aforementioned improvements on model structure, different dependencies of 1-RC model parameters can be calibrated over a whole battery operating range to enhance model accuracy and robustness.

In [26,27], a 1-RC model incorporating the Butler–Volmer equation (BVE), as shown in Figure 9, is proposed to take into account the current dependency on charge transfer resistance, due to the outstanding discharge capability of lithium-ion batteries. The BVE describes the nonlinear relationship between overpotential and current in a charge transfer process; thus, the growing trend of battery polarisation voltage can be better reproduced via the proposed model at a large load current. However, the application of the BVE remarkably raises the computational complexity of SOP estimation, which generally requires a numerical method to solve the peak current estimation and, thus, demands strong computational power from BMSs.

In [28], a so-called migrated 1-RC model, as shown in Figure 10, is proposed to improve the robustness of SOP estimation against uncertainties from battery aging and temperature variation, where the model parameters are all characterized as three-dimensional surfaces of SOC and temperature.

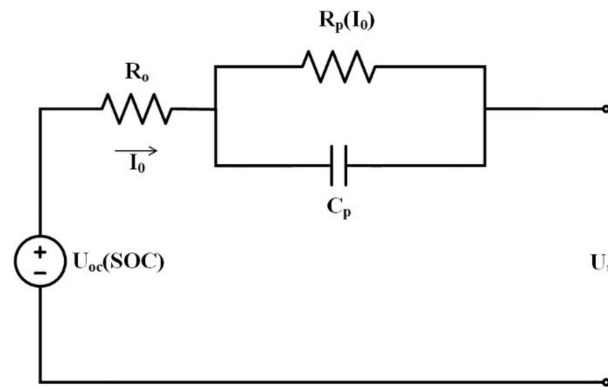


Figure 9. 1-RC model incorporating Butler-Volmer equation [26,27].

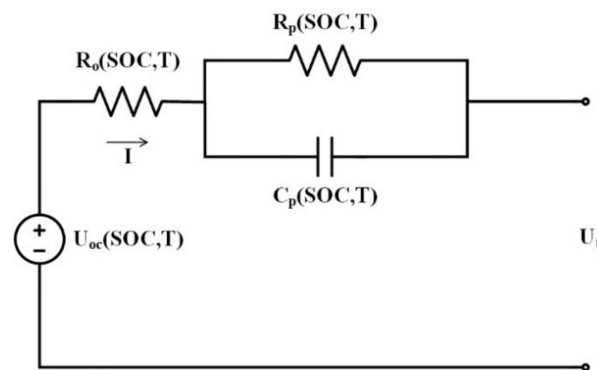


Figure 10. Migrated 1-RC model [28].

Two particle filtering-based linear migrations are devised to adjust model parameters over battery lifetime. However, they totally require 10 migration coefficients to be tuned in parameters recalibration, thereby producing a heavy computational burden for BMSs in EV applications.

In [29], an improved 1-RC model with multi-dependent OCV, as shown in Figure 11, is established for SOP estimation, in order to compensate the distortion phenomenon of OCV-SOC curve. The multi-dependent OCV, is modelled as a multi-dimensional map of SOC, temperature, aging factor, and hysteresis factor to adapt complex load conditions, which is advantageous to both online SOC and SOP estimation.

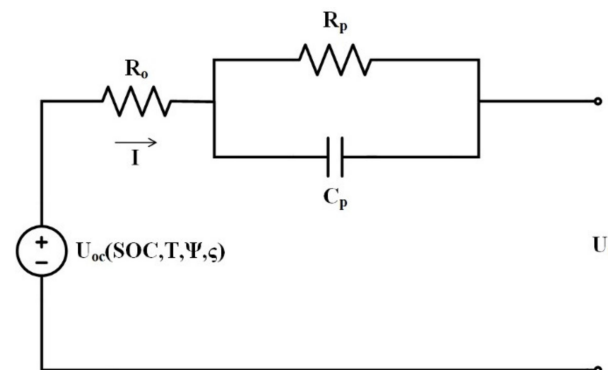


Figure 11. 1-RC model with multi-dependent OCV [29].

For the readers' convenience, the benefits and drawbacks of the improved 1-RC models have been listed in Table 1.

Table 1. Benefits and drawbacks of the improved 1-RC models in online SOP estimation.

	Improved 1-RC Models	Benefits	Drawbacks
Structure improvements	1-RC model with diffusion resistance [19]	<ul style="list-style-type: none"> • Enhance the model accuracy in describing diffusion process • Remain low model complexity 	<ul style="list-style-type: none"> • Require a mass of tests to model diffusion resistance • Lack of robustness
	1-RC model with one-state hysteresis [20–23]	<ul style="list-style-type: none"> • Offset hysteresis voltage 	<ul style="list-style-type: none"> • Increase model complexity • Increase computational cost in SOP estimation
	1-RC model considering self-discharge phenomenon [24]	<ul style="list-style-type: none"> • Enhance the model robustness against battery calendar aging and cycling aging 	<ul style="list-style-type: none"> • Require a mass of data to establish battery aging model • Lack of robustness under different driving experience
	1-RC model with a moving average noise [25]	<ul style="list-style-type: none"> • Enhance the model accuracy under dynamic load profiles • Barely increase the computational cost in SOP estimation 	<ul style="list-style-type: none"> • Increase model parameters • Model accuracy depends on the length of the moving horizon
Consider parameter dependencies	1-RC model incorporating Bulter-Volmer equation [26,27]	<ul style="list-style-type: none"> • Enhance the model accuracy against current effect 	<ul style="list-style-type: none"> • Largely increase model complexity • Increase computational cost in SOP estimation
	Migrated 1-RC model [28]	<ul style="list-style-type: none"> • Enhance the model accuracy against the effects of SOC and temperature 	<ul style="list-style-type: none"> • Require a mass of tests to extract parameter dependencies • Largely increase model parameters
	1-RC model with multi-dependent OCV [29]	<ul style="list-style-type: none"> • Enhance the model robustness of OCV-SOC curve against the effects of temperature, hysteresis and battery aging 	<ul style="list-style-type: none"> • Require a mass of tests to extract parameter dependencies • Increase model parameters

3.1.2. Other Models

Apart from the improved variants from the basic 1-RC model, some other ECMs have also been employed to achieve the favourable performance in online SOP estimation.

R_{int} model is the simplest ECM, by ascribing the whole battery internal voltage response to an internal resistance and is generally employed in instantaneous SOP estimation. Nevertheless, the internal resistance features high-dynamic characteristic and can be largely affected by multiple factors, such as SOC, current, and temperature. Thus, it is up to the need for a R_{int} model to determine which factor will be taken into account in the internal resistance.

In [30], a multi-dependent R_{int} model, as shown in Figure 12, is constructed for online instantaneous SOP estimation that considers the effects of SOC and current on the internal resistance. Their correlations are calibrated offline by performing pulse tests at various SOC and current amplitudes. After that, fuzzy rules are adopted to realize online feature mapping of the internal resistance for instantaneous SOP estimation.

In [31,32], the thermal effect on battery instantaneous SOP is investigated based on a multi-dependent R_{int} model. Their experimental results show a positive correlation between battery instantaneous peak power and temperature. Besides, an empirically-derived temperature correction term is devised in [31] to further facilitate model robustness at extreme temperatures, which guarantees 95% confidence interval in instantaneous SOP estimation from $-20\text{ }^{\circ}\text{C}$ to $50\text{ }^{\circ}\text{C}$. The improved accuracy of online instantaneous SOP estimation at different temperatures can, therefore, be achieved.

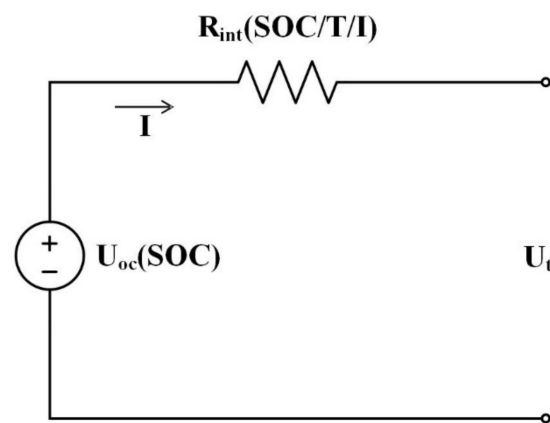


Figure 12. Multi-dependent Rint model [30–32].

As a major limitation of R_{int} model and its modified versions, the existence of battery polarisation voltage cannot be properly reflected in SOP estimation under dynamic loads. In view of this, a linear regression model, as shown in Figure 13, is proposed in [33]. Instead of using any specific electrical components, battery polarisation voltage is comprehensively described in a linear regression form, with respect to a past current sequence. By virtue of linear regression, the online parameters identification of this model contributes to the ease of implementation, and the peak discharge and charge current in the CC mode can be easily expressed. Moreover, a trade-off has to be made for the proposed model between the memory length and number of its coefficients, where extending memory length could attain a better tracking capability of battery nonlinearity but at the cost of identifying more coefficients.

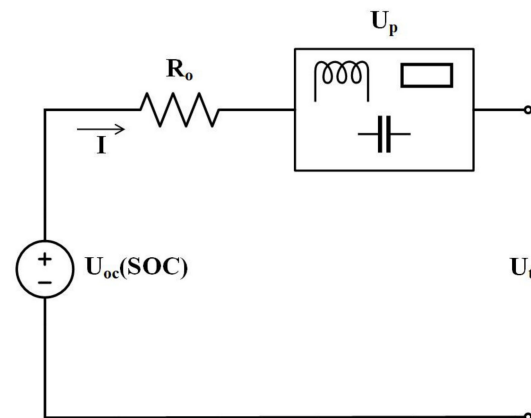


Figure 13. Linear regression model [33].

The dual polarisation (DP) model, as shown in Figure 14, is another widely used ECM in SOP estimation [34–39]. Compared with the 1-RC model, the DP model takes advantage of two RC networks with different time constants to describe the charge transfer process and double-layer effect at the mid frequency region, as well as the diffusion phenomenon at the low frequency region, thereby showing the improved model accuracy over basic 1-RC model, especially at extreme SOC regions [40].

In [34,38], a DP model is associated with a two-state thermal model to reproduce battery electrical and thermal dynamics. The thermal effect inside a battery on model parameters can be reflected in real-time, aiming to enhance the robustness of SOP estimation at varying temperatures. In [35], a multi-constraint SOP estimation is implemented, based on a DP model. The authors evaluate the performance of the DP model with adaptive model parameters in SOC estimation, which demonstrates a SOC error of less than 2%, compared to 3% of a basic 1-RC model over a whole battery operating range. However, the experimental validation of the DP model in SOP estimation was not directly performed.

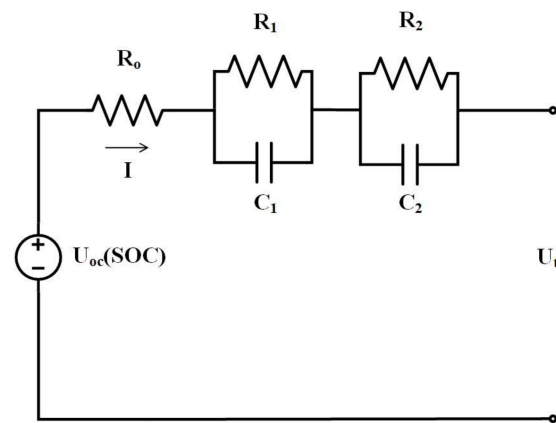


Figure 14. Dual polarisation model [34–39].

Due to the fact that integral order models with ideal resistors and capacitors are incapable of accurately capturing the frequency domain impedance of lithium-ion batteries, a number of fractional order models have been devised for SOP estimation. In [41], a simplified fractional order model, comprising of an ohmic resistance and a Warburg element, is proposed for SOP estimation, as shown in Figure 15.

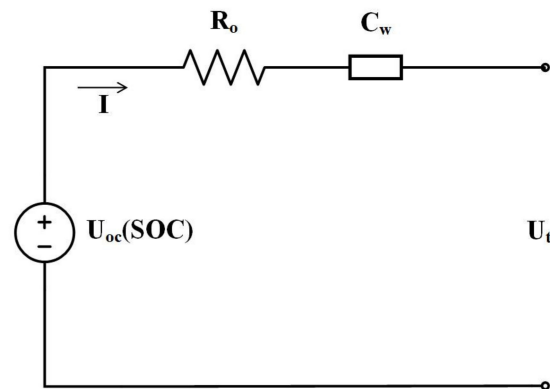


Figure 15. Simplified fractional order model [41].

As most EV driving cycles are concentrated at low frequency region (<1 Hz), the RC network in a basic 1-RC model is simplified to a linear resistance, while a Warburg element is added to describe battery diffusion phenomenon at the low frequency region. Besides, according to the Grünwald–Letnikov definition and short-memory principle [42], the complicated nonlinear dynamics of the Warburg element are in relation to all of its historical states and load current within a memory horizon, which pose a challenge in battery peak discharge and charge current estimation. In light of this, the authors decompose the voltage response on Warburg element into zero-input and zero-state responses, leading to the simplification of the nonlinearity of Warburg element. Although the proposed model could generate a concise expression for peak current estimation, it sacrifices the model nonlinearity (in describing battery relatively fast dynamics).

With that in mind, an improved fractional order model, with two serial-connected resistor-constant phase element (RC_{CPE}) networks, is proposed in [43] for the better reproduction of battery internal dynamics over a broad-frequency domain, as is shown in Figure 16. The increased model complexity is of benefit to model accuracy; however, it is considerably cost-intensive to solve the peak discharge and charge current in real-time. To promote the applicability in real applications, only the initial state in a memory horizon will pose an effect on the battery electrical behaviour at the end of a prediction window, while the other states in-between are omitted. On the other hand, it may adversely affect the model accuracy of the employed fractional order model.

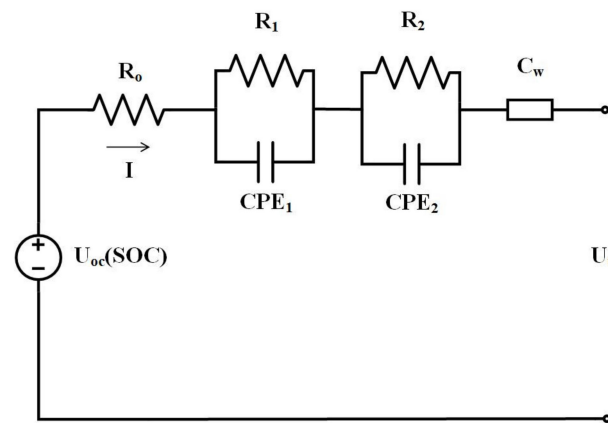


Figure 16. 2-RC fractional order model with a Warburg element [43].

Additionally, the comparative studies among ECMs with different numbers of RC, RC_{CPE}, or resistor-Warburg element (RC_W) network, in series, were carried out in [44,45] to examine their performances in online SOP estimation. The schematic diagram of model structure is displayed in Figure 17.

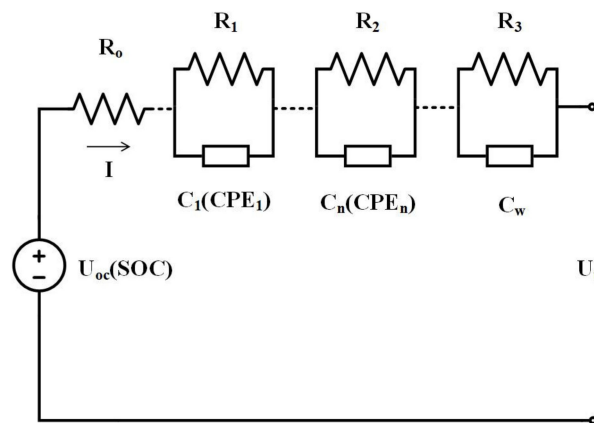


Figure 17. n-RCW integral and fractional order models [44,45].

In [44], the authors compare the model accuracy of seven ECMs with a number of RC or RC_{CPE} networks, ranging from 0 to 3, under different operating conditions. The electrochemical impedance spectroscopy (EIS) method is implemented, in a range from 5 k Hz to 1 m Hz, for parameters identification over a whole SOC range, while a hybrid pulse power characterization (HPPC) test is performed to capture battery impedance characteristics and peak power capability for validation. A particular emphasis is laid on investigating the current dependence on the parallel resistance in RC or RC_{CPE} networks. A similar research is presented in [45], with an intention to figure out the optimal ECM for online SOC and SOP estimation. The experimental outcomes reveal that the increasing number of serial-connected RC and RC_{CPE} networks would be conducive to model accuracy. Meanwhile, fractional order models outperform integral order models with the same structure in SOC and SOP estimation, over a whole battery operating range. Further, considering the trade-off between model accuracy and computational complexity, the fractional order model with one RC_{CPE} network and one RC_W network is observed as the optimal ECM in SOC and SOP estimation, with an error of less than 2%, under all the dynamic current profiles.

The benefits and drawbacks of other models with different structures to the 1-RC model, with its variants in online SOP estimation, have also been summarised and presented in Table 2.

Table 2. Benefits and drawbacks of other models with different structures from 1-RC model and its variants in online SOP estimation.

Other Models	Benefits	Drawbacks
Multi-dependent R_{int} model [30–32]	<ul style="list-style-type: none"> • Simple structure and low model complexity 	<ul style="list-style-type: none"> • Require a mass of tests to capture parameter dependencies • Incapable of describing battery polarisation state
Linear regression model [33]	<ul style="list-style-type: none"> • Low computational cost 	<ul style="list-style-type: none"> • Model accuracy depends on the length of previous state
Dual polarisation model [34–39]	<ul style="list-style-type: none"> • Relatively high model accuracy 	<ul style="list-style-type: none"> • Have trouble describing diffusion process
Simplified fractional-order model [41]	<ul style="list-style-type: none"> • Simple structure • Capable of describing diffusion process 	<ul style="list-style-type: none"> • Relatively high computational cost • Incapable of describing battery charge transfer process
2-RC fractional-order model with a Warburg element [43]	<ul style="list-style-type: none"> • High model accuracy 	<ul style="list-style-type: none"> • High model complexity • High computational cost
n-RCW integral- and fractional-order models [44,45]	<ul style="list-style-type: none"> • High model accuracy 	<ul style="list-style-type: none"> • High model complexity • High computational cost

3.2. Improved Online Parameter Identification Technique

Model parameters of a battery feature slow-varying characteristic and are jointly influenced by a series of factors (e.g., SOC, current, and temperature). Considering the accuracy, adaptability, and computational efficiency for EV applications, online parameter identification techniques offer more superiority over offline techniques, which could only be implemented in a laboratory environment and may gradually lose fidelity during service. By far, online parameter identification techniques can be divided into two main groups: recursive and non-recursive methods [46].

Because of strong adaptability and low computational effort, recursive methods, such as the recursive least-square (RLS) algorithm and Kalman filter (KF) family, are favoured as the preferred candidate for model parameterisation in SOP estimation. On the other hand, this type of methods requires model mathematical expression to be converted into a linear regression form, with respect to model parameters and measurable signals, which may not be suitable for some ECMs with high nonlinearity. In [47], the authors proposed a RLS algorithm with an adaptive ratio vector for online model parameterization in pack-level SOP estimation. The RLS algorithm is employed to provide mean parameters estimation at a pack level, while cell inconsistencies are evaluated through the adaptive ratio vector, based on the analysis of cell current–voltage characteristic. In [13,19], a weighted RLS (WRLS) algorithm is employed in online parameters identification for SOP estimation, where a larger weight factor of an error gives rise to more impact on parameters adjustment. It should be noted that weight factors in a recent past window could exert an influence on the regression of the algorithm, and the optimisation of these weight factors is strongly related to the sampling rate and load profile. In [48–50], an optimal forgetting factor RLS (FFRLS) algorithm is implemented to determine model parameters by minimizing the accumulated squared error and updating progressively with data collections. A proper forgetting factor could effectively provide more impact of recent data than past data on the fine-tuning of model parameters, thereby acquiring better tracking ability and numerical stability. In [29], an adaptive forgetting factor least-square (AFFLS) algorithm is proposed to capture parameters variation in estimation of SOC and SOP, where the adaptive forgetting factor is designed to be current-dependent to compensate for the nonlinear correlation between charge transfer resistance and current. In [51], an improved AFFLS algorithm is developed to achieve preferable performance in processing fluctuated data, while simplifying preliminary experimental analysis and data fitting, thereby enhancing its

operability in online SOP estimation. In [52], the authors emphasize that the unexpected sensing noises in current and voltage signals may cause biased parameters identification and further affect SOC and SOP estimation accuracy. Therefore, an adaptive forgetting factor recursive total least square (AFFRTLS) algorithm is proposed to suppress the current and voltage corruptions by finding out the optimal solution with the minimum perturbation on a battery system. According to the experimental results, the proposed algorithm presents a SOC error of less than 2.7% against sensing noises, while the error is up to 5% using a FFRLS algorithm.

The KF family is another important recursive method that shows an advantage in either the joint or dual estimation of both model parameters and state variables of a battery system [53]. In a joint estimation strategy, the state vector of a battery system is augmented to include model parameters, one KF is used to estimate both battery parameters and states to improve the computational efficiency. In [54], battery OCV is treated as a state variable instead of SOC in this algorithm to provide the basis for SOP estimation, and an offline calibrated curve, in relation to the rate of OCV change per ampere-hour, is employed to achieve close-loop compensation. However, the initial values of the KF are required to be well chosen to ensure convergence. In [55], to jointly estimate battery model parameters and state variables, while considering current dependency on charge transfer resistance, the fully-polarised internal resistance is calibrated at various current amplitudes and treated as an observation in an unscented KF (UKF). By doing so, it enables a viable way to capture the current effect for online SOP estimation while avoiding constructing a BVE-based highly nonlinear model. In [41], a fractional KF algorithm is employed to realise the joint estimation of battery states and model parameters of a simplified fractional order model, where the state covariance prediction is associated with the previous state in a memory horizon, instead of only the last one.

As for a dual estimation strategy, two KFs are placed in parallel to act as state and weight filters, to concurrently share the derived information of state variables and model parameters with each other [53]. Although the dual strategy demonstrates a relatively complex structure, it could avoid large matrix operation in a joint estimation strategy and, thus, relieve the computational burden. In [14,37], both battery model parameterization and online SOC estimation are implemented using a dual EKF (DEKF) algorithm. In [14], the proposed DEKF algorithm employs battery polarisation current, flowing through the charge transfer resistance of a 1-RC model as the state vector, and incorporates battery OCV into parameter vector. As a benefit, the partial derivative in DEKF algorithm can be simplified. According to the experimental validations on a new and aged cell, the estimated voltage error can be restricted within 0.03 V against noise. In [37], a pseudo-random binary sequence (PRBS) is applied to recalibrate parameters by exciting batteries during a relaxation, which delivers a reliable prior knowledge to an EKF for subsequent online adaptation. According to the validations, the proposed hybrid parameters identification method exhibits higher accuracy and faster convergence speed than EKF algorithm without prior knowledge, indicating the significance of prior knowledge for regression-based algorithms. In [56], cell parameters and SOCs in a battery pack are concurrently estimated through a dual adaptive EKF (DAEKF) algorithm, which has a stronger convergence capability than EKF algorithm by regressing noise covariance iteratively. Then, the weakest cell will be identified for pack-level SOP estimation.

Additionally, the extremum seeking algorithm, as another typical recursive method, is employed in [22] to characterize model parameters for instantaneous SOP estimation, where a sinusoidal current signal is imposed on a battery system to generate a cost function. The estimated model parameters will converge to true values, as long as the cost function is approaching zero.

Non-recursive methods, such as optimisation algorithms, possess good accuracy and stability over recursive methods, especially for ECMs with complex structures and more parameters. However, these methods are generally computationally expensive and require processing batches of data simultaneously. In [27], the parameters of a 1-RC

model, incorporating the be, are updated online at the interval of 10 s, through an optimal searching strategy. The basic idea is to select a reference parameter set, among a number of the randomly generated parameter sets, at each iteration, according to the accumulated squared voltage error [57]. In [58], a particle swarm optimisation (PSO) algorithm is employed in online parameters identification for SOP estimation. Due to slow-varying characteristic of model parameters, it is not necessary to implement PSO algorithm at each sampling time, thereby alleviating its computational effort. From the experiments on nine different cells, PSO algorithm outperforms RLS algorithm in battery voltage and SOC estimation.

3.3. Improvements on SOP Estimation Methods

3.3.1. Long-Term SOP Estimation

Model parameter variation needs to be considered in a lengthy prediction window to maintain model accuracy in SOP estimation against varying SOC. This will lead to the increased computational complexity in solving peak currents online at CC, CV, and CCCV modes.

In [59], the ohmic resistance of a 1-RC model is predicted forward in a prediction window using the first-order Taylor series expansion. As a result, the mathematical expression of the peak discharge current becomes a second-order polynomial, and an optimal searching algorithm is designed to seek peak discharge current, while peak charge current estimation is not involved. To further engage all model parameters in forward prediction, the same authors employed a genetic algorithm (GA) to work out the peak discharge and charge currents from a highly nonlinear function; additionally, the effects of erroneous SOC and battery aging on SOP estimation were systematically analysed [60]. In [61], the authors stated that the first-order Taylor series expansion may yield unrealistic estimations of model parameters (e.g., negative values) at the end of a prediction window. To tackle this issue, a voltage, limited by an extrapolation of resistances and OCV (VLERO) method, is proposed by extrapolating the model parameters on a slope connected between the present and minimum values over a whole SOC range. Moreover, a multistep model predictive iterative (MMPI) algorithm was derived to achieve SOP estimation in high accuracy, which can be separated into an inner and outer stages. In the inner stage, a prediction window is segmented into several subintervals to capture the variation trend of polarisation voltage in great detail, based on the model parameters estimated at each end of the subinterval. A root-searching algorithm is performed in the outer stage to find out the exact peak current from a complex function. The proposed MMPI algorithm is validated under dynamic profiles at low temperature, which shows a much preferable performance to a conventional long-term SOP estimation at the CC mode.

3.3.2. Optimisation Control-Based SOP Estimation

SOP estimation can also be converted into an optimisation problem using control theory. In [62], a dynamic matrix control (DMC) algorithm, developed from the model predictive control (MPC) theory, is applied in SOP estimation. Battery terminal voltage is formulated as a linear combination of the weighted sum of current changes in a recent past window. Thus, the proposed algorithm optimises the power flow through a tuning load current to make a battery reach its cut-off voltage at the end of a prediction window. In [34], an economic nonlinear MPC algorithm is employed in SOP estimation, under the constraints of voltage, current, SOC, and temperature. Compared with conventional MPC and DMC algorithms, mainly designed for tracking purpose, the proposed algorithm could avoid laborious weight-tuning work and achieve improved close-loop performance, especially targeting the nonlinear system. Besides, the effects of temperature, the length of a prediction window and model accuracy on SOP estimation are quantitatively explored. The experimental results show the error of peak power estimation is less than 0.2%.

Fuzzy logic control theory can be also applied in SOP estimation. In [63,64], a fuzzy logic controller is designed to prevent batteries from breaching the pre-set constraints and

guarantee the safe operation of lithium-ion batteries. SOP estimation outcomes, provided by a MPC algorithm at CC or CCCV modes, will be delivered to a fuzzy logic controller, which divides the safe operating area into an inner and outer region. Once battery terminal voltage or current enters into the outer region at a sudden load change, the fuzzy logic controller will commence the adaptation process before a battery approaches its pre-set constraints, where the correction coefficient depends on battery voltage and current, along with their variation rates.

3.3.3. SOP-Related Multi-State Co-Estimation

Generally, SOC, reflecting the ratio of battery remaining capacity to its rated capacity, is regarded as the indispensable precondition for SOP estimation. Many joint SOC and SOP estimation methods have been reported in the literature. With in-depth studies on lithium-ion batteries, it was found that the multi-physics coupling effect among various battery states could impose a significant impact on the estimation performance of every single state. Therefore, SOP-related, multi-state estimation becomes a promising way to facilitate SOP estimation in practice and has been a research hotspot in recent years. The relevant methods will be reviewed, with a special emphasis on the contributions of SOE and SOH to SOP estimation.

As one of the most fundamental battery states of lithium-ion batteries, SOE describes the ratio of battery remaining energy to its rated energy, which is closely related to EV remaining driving range estimation. From an energy management standpoint, it could also offer batteries a constraint in SOP estimation to prevent them from falling into energy poverty quickly. In [65], SOE completely supersedes SOC to act as a constraint in SOP estimation. According to the authors, SOE limit could have a higher impact on SOP estimation than SOC limits, since battery internal energy dissipation in a prediction window cannot be reflected by SOC, from a charge accumulation perspective. In [21], multi-state estimation algorithms, including SOC, SOE, and SOP, are presented, based on a 1-RC model with hysteresis. Although SOE is a state variable in battery state space model, it does not participate in the model observation equation, which is estimated in an open-loop fashion. However, the above two methods ideally assume battery terminal voltage to be constant in a prediction window, which is practically untrue and, thereby, provides over-optimistic estimation results. Moreover, it is a necessity to experimentally investigate the battery operating ranges that SOC and SOE limits would, respectively, come into effect in SOP estimation, before completely replacing SOC limit with SOE limit.

SOH is a measure of the fade of battery capacity or increase of battery internal resistance, compared with a fresh battery. It can be calculated as a ratio of the maximum battery capacity at its current state to its rated capacity or the ratio of the internal resistance at its current state to the internal resistance at a fresh battery. Unlike the contribution of SOE, SOH estimation mainly dedicates to model parameters recalibration against battery degradation, thereby improving the SOC and SOP estimation accuracy over battery lifetime. In [36], a multi-state estimation framework of SOC, SOH, and instantaneous SOP was developed for lithium-ion batteries in EVs. A DP model, with offline characterized SOC- and temperature-dependent model parameters, was employed in SOC estimation, while the estimations of SOH and instantaneous SOP shared a R_{int} model. The SOH estimation in this research only helps recalibrate the available battery capacity, battery aging effect on the other model parameters is not taken into consideration, which would affect SOC estimation in the long run. Further, the employment of two ECMs with different structure and parameters reduces the applicability in practice. Another multi-state estimation framework of SOC, SOH, and SOP is proposed in [66], where SOH will be updated quarterly or semi-annually, based on the charge accumulation between two separate SOC. Thus, the degradation trend of available battery capacity can be captured, yielding the improved performance of SOP estimation at the CCCV mode. A similar SOH update mechanism is also applied in [39]. Besides, the authors discovered that the OCV-SOC curve barely drifts above 62.5% SOC over a whole battery lifetime in EVs (i.e., 80–100% SOH), with a

voltage deviation of less than 0.005 V. In this regard, two separate SOC levels will be selected, in a range above 62.5% SOC. To further illustrate the correlation among SOC, SOH, and SOP, an enhanced multi-state estimation hierarchy is proposed in [8], where SOC estimation provides the basis for SOH and SOP estimation. SOH estimation is at the mid-layer, which can help to improve model robustness for SOP estimation and recalibrate SOC estimation against battery aging. The top layer of the hierarchy is a SOP estimation that could attain high reliability, benefiting from the precise knowledge of both SOC and SOH. Three length-varying rolling windows are designed for model parameters identification, SOH estimation, and SOP prediction, respectively. First, a modified moving horizon estimation (MHE) algorithm, with enhanced numerical stability and fault tolerance, is employed in SOC estimation. Second, periodical updates of model parameters and SOH will further lead to improved accuracy in SOC estimations. By doing so, a newly defined current limit, focusing on an increased heat generation on ohmic resistance in an aged battery, can be introduced into SOP estimation for safety consideration. The experimental results validate the effectiveness of the proposed multi-state estimation for SOC, SOH, and SOP of cells at different aging statuses. In [67], the multi-state estimation algorithm, with respect to SOC, SOH, and SOP, was proposed, primarily based on the mixed SOH estimation strategy. In this proposed algorithm, a 3-RC model was constructed, with parameters calibrated on a battery at different aging states, while an interacting multiple model strategy is applied to evaluate the respective mode probabilities, based on the corresponding likelihood functions. According to the aging states of the pre-defined models and their mode probabilities, the first SOH candidate can be generated. In addition, the online identified ohmic resistance is treated as the second candidate of SOH. The overall SOH estimation can be determined by taking a weighted average between two candidates, thereby achieving a smooth mode transition and benefiting from more stable SOP estimation.

3.3.4. Machine Learning-Based SOP Estimation

Machine learning algorithms exhibit outstanding performance in nonlinear system modelling, some of them with simple structure, and few parameters have been attempted in SOP estimation for the improved accuracy, while keeping a relatively low computational expense. In [68], a self-learning estimation algorithm was proposed for SOP estimation, based on an adaptive neuro-fuzzy inference system (ANFIS). The proposed ANFIS treats the current amplitude, charge accumulation, SOC, temperature, and time-averaged voltage during a pulse as the system inputs, while the system output is the battery terminal voltage at the end of a prediction window. A two-step hybrid learning method is employed in ANFIS training. In the first step, a forward pass is performed with fixed premise parameters to generate the corresponding output error. Then, a gradient descent-based back pass is carried out in the second step to fine-tune the premise parameters. Finally, the peak discharge and charge current/power is determined by iteratively running the system, and the estimation will gradually approach the peak value through a bisection method. In [69], a model-based extreme learning machine (ELM) algorithm was derived to predict battery future power capability, voltage, and temperature against varying SOC and temperature. The proposed ELM algorithm replaces original active functions in conventional ELMs with a set of sub-models. Each of these sub-models contains a 1-RC model and thermal model, with randomly selected initial SOC and model parameters in a reasonable range to reproduce battery electrical and electrothermal dynamics. As an advantage, little *priori* knowledge of a battery is required, thereby facilitating the robustness of the algorithm. According to the experimental results at 5 °C, 25 °C, and 45 °C, the proposed algorithm performs satisfyingly over the generic RLS algorithm.

3.3.5. Pack-Level SOP Estimation

EV battery packs are made up of numerous cells connected in series or parallel (or combination of both) to meet specific power and energy requirements. Thus, pack-level SOP estimation appears to be subjected to all cell-level constraints. The fundamental idea

of the conventional pack-level SOP estimation is to predict the SOP of a single cell and then scale it up to the whole battery pack. Nevertheless, cell inconsistencies are inevitable in the process of manufacturing and usage. Neglecting cell inconsistencies in a battery pack may yield unreliable SOP estimation outcomes. As a result, it could aggravate battery aging behaviour and even risk batteries in potential safety issues. Generally, serial or parallel connections are two common configurations to make a battery pack [70].

For a battery pack comprising of only serial-connected cells, pack-level SOP depends on the representative cell that first reaches any of the pre-set constraints [71]. A straightforward strategy to determine the representative cell in a battery pack is proposed in [20,72] by comparing the peak cell currents in a prediction window. However, this strategy requires a large memory from BMSs to construct ECMs for each single cell and store the corresponding parameters. Also, working out all the peak cell currents would produce a heavy computational burden on a microprocessor with limited computation capability. To facilitate the applicability and efficiency of pack-level SOP estimation, an improved cell-selection strategy was devised in [56], based on the extraction of cell inherent features (e.g., OCV and ohmic resistance), which enables to pick the representative cell before implementing the peak current estimation. Although laborious computational effort on calculating peak cell currents can be avoided, it still requires cell-level modelling and the corresponding estimators for cell parameter identification. In light of this, a comprehensive model is constructed to describe dynamic behaviours of a battery pack, while cell-to-cell differences are reflected by a set of proportional factors that replace cell inherent features (e.g., cell capacity and ohmic resistance) in representative cell selection [27,47]. Afterwards, the peak discharge and charge currents of the representative cell cooperate with the average cell voltage to generate pack-level SOP. As an advantage, it only needs one estimator to suffice for the parameter identification at a pack level that further saves computational resources.

The aforementioned SOP estimation strategies are readily applicable to a serial-connected battery pack, which do not consider the presence of parallel-connected cells. Unlike serial-connected battery packs that share an identical current, dynamic current distribution would be the most intractable problem for SOP estimation of a battery pack in a parallel-connected structure. Concerning this, an application-oriented SOP estimation strategy was proposed in [5] for a battery pack constituting parallel-connected strings with a number of cells connected in series on each string. Firstly, a generalised state-space representation of a n-RC model is constructed to describe battery internal dynamics, which treats either cell voltage or string current as a system output, with the pack current as a system input. This makes the complicated system much easier to monitor. Secondly, the SOP estimation is formulated as an optimisation problem that not only searches the cell index hitting the pre-set constraint but also determine the exact time instance, since a possible non-monotonic variation of cell voltage may occur, in spite of operating at a constant current. Further, cell SOPs at the beginning and end of a prediction window will be tried before solving the optimisation problem to reduce the computational effort.

For the readers' convenience, the reviewed SOP estimation methods are demonstrated and compared in Table 3, where the corresponding evaluation methods are particularly focused.

Table 3. Improved SOP estimation methods at different operating modes.

Research Emphasis	References	Methods	Operating Mode	Special Considerations
Long-term SOP estimation	[59]	Optimal searching algorithm	CC mode	Future prediction of R_0
	[60]	GA	CC mode	Future prediction of R_0 , R_p and C_p
	[61]	Modified VLERO and MMPI methods	CC mode	Future prediction of R_0 , R_p and C_p
			CC mode	
Optimisation control-based SOP estimation	[62]	DMC	CC mode	–
	[34]	Economic MPC	CC mode	Temperature acts as a constraint
	[63]	MPC and fuzzy control	CC mode	–
	[64]	OLPM and fuzzy control	CC mode	–
			CCCV mode	

Table 3. Cont.

Research Emphasis	References	Methods	Operating Mode	Special Considerations
SOP-related multi-state co-estimation	[21,58,65] [8,36,39,67] [66]	OLPM OLPM OLPM	CC mode CC mode CCCV mode	SOE acts as a constraint SOC, SOH and SOP estimation SOC, SOH and SOP estimation
Machine learning-based SOP estimation	[68] [69]	ANFIS ELM	CC mode CC mode	– –
Pack-level SOP estimation	[5] [56] [70] [71]	OLPM OLPM OLPM OLPM	CC mode CC mode CC mode CC mode	Parallel-connected battery pack Serial-connected battery pack Serial-connected battery pack Serial-connected battery pack

4. SOP Testing Methods

A high-precision acquisition of SOP reference value is critical for the quantitative evaluation of SOP estimation algorithms. However, there is not a standard and uniform testing method to validate the effectiveness of SOP estimation, and the existing methods are generally carried out at a CC, CV, or CCCV mode to simulate the extreme driving conditions of EVs in a pre-defined prediction window for the measurement of reference SOPs. To this end, the SOP testing methods are reviewed in this section, and their benefits and drawbacks are summarised in Table 4. In the following, we take a battery to conduct SOP test in a prediction window of 10 s as an example for illustration.

Table 4. Existing SOP testing methods and their benefits and drawbacks.

Validation Objective	SOP Testing Method	References	Benefits	Drawbacks
SOP at CC mode	HPPC test	[11,20,36,66,67]	<ul style="list-style-type: none"> Ease of implementation High efficiency 	<ul style="list-style-type: none"> Over-estimated outcomes Improper for long-term SOP measurement Only consider voltage limit
	Hybrid pulse test	[73]	<ul style="list-style-type: none"> Ease of implementation High accuracy 	<ul style="list-style-type: none"> Low efficiency Extrapolation of test data may affect accuracy
	Constant voltage constant power test	[45,74]	<ul style="list-style-type: none"> Relatively good efficiency 	<ul style="list-style-type: none"> Improper to represent real SOP at a CC mode
	Constant current test	[43]	<ul style="list-style-type: none"> Ease of implementation Relatively high accuracy 	<ul style="list-style-type: none"> Low efficiency Nonlinear fitting of test data may affect accuracy
SOP at CV/CCCV mode	Constant voltage test	[13,14,64,66]	<ul style="list-style-type: none"> High accuracy 	<ul style="list-style-type: none"> Require test equipment to generate a rapid increasing pulse with large amplitude

4.1. Hybrid Pulse Power Characterization Test

The HPPC test is widely employed in battery instantaneous and short-term SOP validations [75]. A complete HPPC test profile, over a whole SOC range, is depicted in Figure 18a. Each HPPC test, at a selected SOC point, comprises of discharge and charge pulses, both of which will last for 10 s, followed by a 40 s relaxation. Figure 18b illustrates the basic idea of HPPC test for validations of instantaneous and short-term SOP estimation. Instantaneous peak discharge power can be calculated by Equation (1), based on the abrupt voltage drop at the beginning of a pulse. The characteristics of instantaneous peak discharge and charge power over a whole SOC range are described in Figure 18c.

$$\begin{cases} R_{\text{int,dis}} = \left| \frac{\Delta V_{\text{dis}}}{\Delta I_{\text{dis}}} \right| = \left| \frac{(V_1 - V_0)}{I_{\text{dis,pulse}}} \right| \\ P_{\text{dis}} = \frac{U_{t,\text{min}}(U_{\text{oc}} - U_{t,\text{min}})}{R_{\text{int,dis}}} \end{cases} \quad (1)$$

For SOP estimation in a short term (<10 s), battery internal resistance is calibrated based on the voltage drop over a whole pulse. Therefore, the peak discharge power, in a short term, can be calculated by:

$$\begin{cases} R_{int,dis} = \left| \frac{\Delta V_{dis}}{\Delta I_{dis}} \right| = \left| \frac{(V_2 - V_0)}{I_{dis,pulse}} \right| \\ P_{dis} = \frac{U_{t,min}(U_{oc} - U_{t,min})}{R_{int,dis}} \end{cases} \quad (2)$$

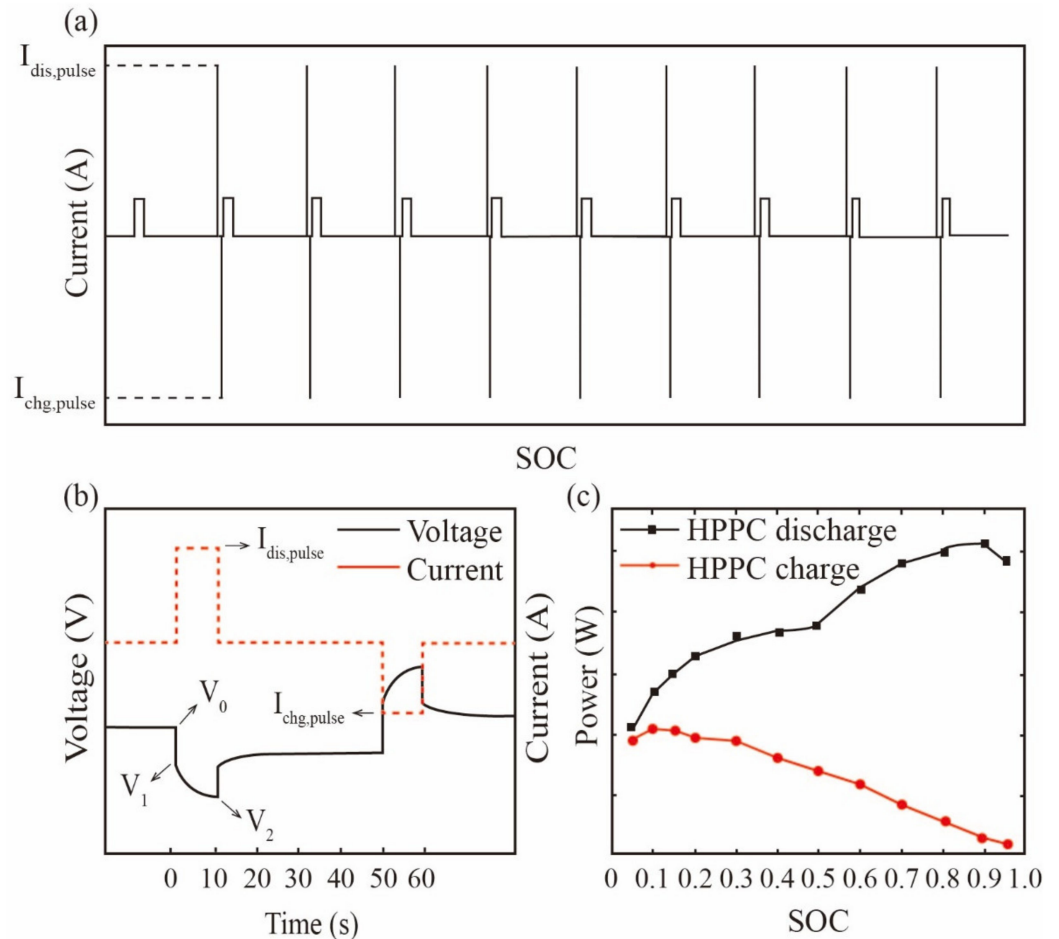


Figure 18. HPPC profile: (a) current profile; (b) typical current sequence and voltage response in a HPPC test; (c) instantaneous peak power through the HPPC test.

Although the HPPC test is a simple method to carry out with a fairly high efficiency, its defects for SOP reference calibration are summarised below:

1. The HPPC test is improper for examining SOP estimation in a relatively long prediction window (>30 s), since battery OCV variation in a pulse is neglected.
2. The HPPC test cannot be performed for dynamic SOP validation, since it must start from a static condition.
3. Equation (2) cannot accurately reproduce battery end-of-pulse internal resistance R_{int} at the real peak currents. This is because battery polarisation voltage indicates a strong nonlinear correlation with the current amplitude, while the real peak currents will be much greater than the applied current in the HPPC test. As a result, the calibrated R_{int} will lead to a significant deviation in SOP reference from the HPPC test.
4. The HPPC test can only validate SOP estimation under voltage limit.

4.2. Hybrid Pulse Test

In [73], a hybrid pulse test is reported for SOP validation. The current and voltage profiles of a typical hybrid pulse test at 80% SOC are depicted in Figure 19a, and the test procedure is illustrated as follows:

Step one. Discharge a battery from a fully charged state to 80% SOC, followed by one-hour relaxation.

Step two. Discharge a battery at a conservative guess of peak discharge current for 10 s, and ensure the end-of-pulse voltage will not breach the voltage limit. Record the released capacity and battery terminal voltage at the end of 10 s.

Step three. Charge back the released capacity to the battery and remain the battery at the same initial SOC, namely 80% SOC, followed by another one-hour relaxation.

Step four. Gradually increase the current amplitude and repeat steps two and three five more times. Plot the attempted currents versus the corresponding battery terminal voltages at the end of 10 s. Fit them using a straight line, as shown in Figure 19b.

Step five. Extrapolate the peak discharge current by extending the fitted line to the lower cut-off voltages.

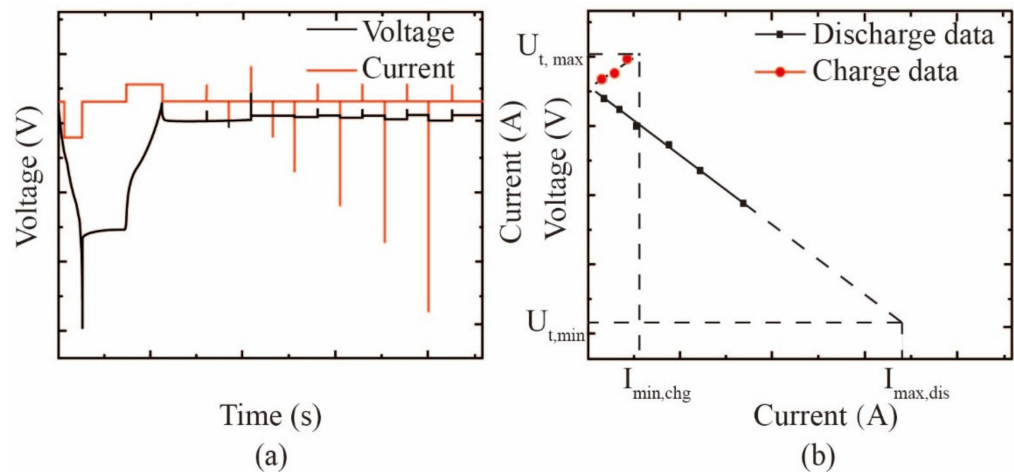


Figure 19. Hybrid pulse test: (a) current and voltage profiles; (b) peak charge and discharge current identification.

A hybrid pulse test could achieve highly accurate SOP with affordable time expense if it satisfies the following conditions:

1. It requires battery end-of-pulse voltage to be close enough to the upper (of lower) cut-off voltage for an accurate extrapolation, since an approximate linear relationship between the attempted current and battery end-of-pulse voltage only appears in a limited range.
2. It requires the discharged capacity in the last pulse test to be charged back to the battery for keeping the same initial SOC before applying the next pulse. However, there will always exist a slight difference in initial OCVs and, thus, SOCs, due to battery hysteresis effect, which may affect the accuracy of the calibrated SOP references.

4.3. Constant Voltage Constant Power Test

Constant voltage constant power (CVCP) test is designed in [45] for SOP validation, which can be separated into CV and constant power (CP) tests. Figure 20 shows the flowchart of the CVCP test. In [74], the authors made a further improvement, where a conception of power sensitivity was proposed to rationally tune the peak discharge and charge power after a CP test. According to the flowchart, SOP reference calibration at a selected SOC can be fulfilled within two battery cycles, indicating a good efficiency for SOP validation. However, SOP references from CP tests may not be a proper way to evaluate

SOP estimation algorithms at the CC or CCCV modes, since the CC mode is essentially different from the CP mode.

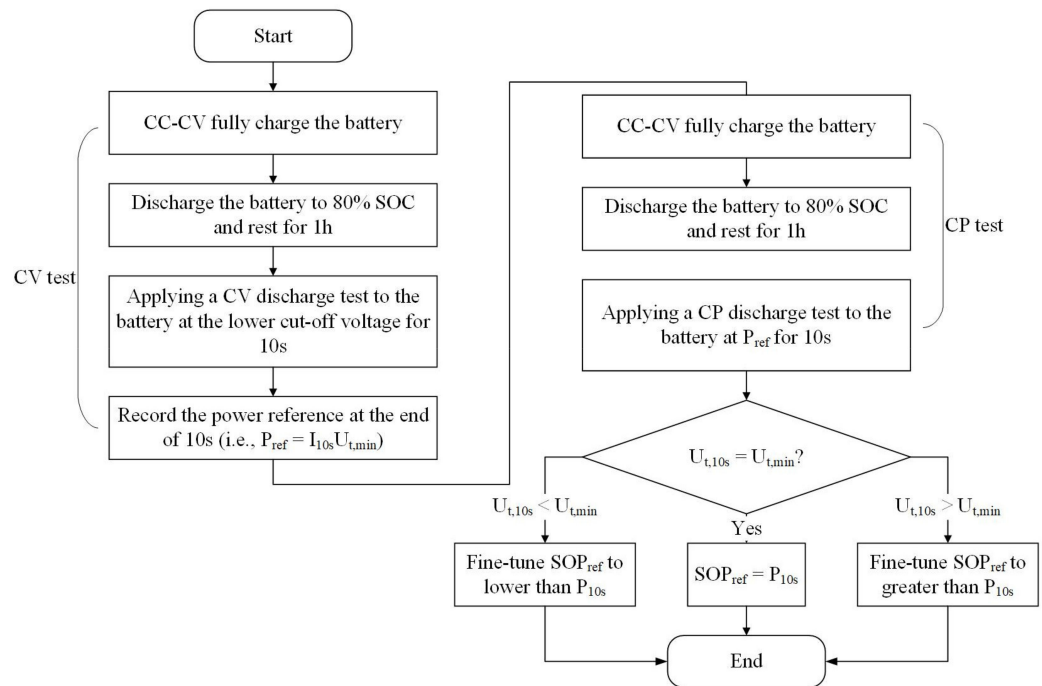


Figure 20. Test flow of the CVCP test at 80% SOC.

4.4. Constant Current Test

In [73], a CC test is proposed for SOP validation. The test procedure is briefed as below:
 Step one. Fully charge a battery and then discharge the battery to 80% SOC, followed by one-hour relaxation.
 Step two. Discharge the battery at the estimated peak discharge current until the battery terminal voltage reaches the lower cut-off voltage. Record the testing time t_1 .
 Step three. Repeat steps one and two four more times at different current amplitudes. Make sure the testing time is approaching the length of a prediction window, namely 10 s.
 Step four. Fit the correlation between the attempted current and recorded testing times as a nonlinear curve. Reference value of the peak discharge current corresponds to $t = 10$ s, as shown in Figure 21.

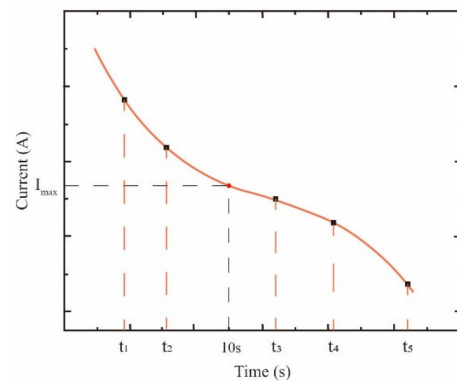


Figure 21. Nonlinear fitting between current and test time in the CC test-based method.

From the test procedures, it can be found that CC test is much more time-consuming than the other aforementioned SOP testing methods. It basically demands five attempts to obtain reference SOP at a selected SOC. Furthermore, a few following factors could cause accuracy deterioration:

1. Different current attempts may not be evenly distributed, which may affect curve fitting.
2. Nonlinear fitting of the recorded data is likely to run into overfitting or underfitting with only five pairs of measurements.
3. Referring to Peukert's law, battery testing time is not proportional to current in a CC discharge profile.

4.5. Constant Voltage Discharge Test

In [14], a CV discharge test is particularly devised for validations of SOP estimation algorithms at the CV mode and CCCV mode, which is illustrated as follows:

Step one. Fully charge a battery and then discharge the battery to 80% SOC, followed by one-hour relaxation.

Step two. Discharge the battery using a rapid increasing pulse, of which the current amplitude will jump to a large value within a very short period (e.g., 0.1 s). Therefore, three cases would happen in a prediction window, as shown in Figure 22.

Step three. Battery peak power at the end of a pulse can be directly calculated as the product of the current limit and voltage at the end of pulse or the product of the voltage limit and current at the end of pulse.

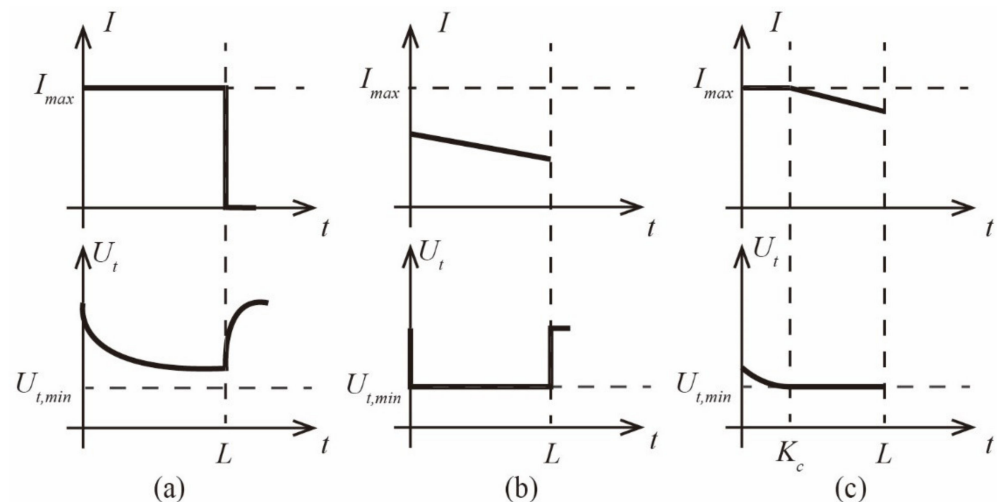


Figure 22. Three cases in a constant voltage discharge test: (a) CC mode; (b) CV mode; (c) CCCV mode.

5. Challenges and Outlooks

Although ECM-based online SOP estimation methods have been rapidly developed in the past decade, with great effort made by manufacturers and researchers in this field, technical challenges are still faced in many aspects. Some recommendations and outlooks of this research are presented in this section for future development.

5.1. Equivalent-Circuit Model

Despite the 1-RC model, with its variants, as a good choice for online SOP estimation, the lack of model accuracy in a broad-frequency band leads to a compromised performance in a lengthy prediction window. In recent years, fractional order models have gained popularity in battery state estimation, owing to their better interpretation of battery electrochemical processes from fast dynamic on the solid electrolyte interface at high frequency regions to charge transfer process and diffusion phenomenon at mid-low frequency regions [76–78]. However, they have not been extensively employed in SOP estimation, and the relevant research is still few. The reason can be ascribed to the highly nonlinear current–voltage characteristics, governed by the short-memory principle that makes the peak discharge and charge currents difficult to be extracted. Besides, fractional order models generally possess more parameters than integral order models and require a large

computational effort to achieve online adaptability, which is another limitation in the application of online SOP estimation. With in-depth research and technical innovation, it can be expected that fractional order models will participate more in online SOP estimation, with increasing computational power of microprocessors in EVs.

Additionally, model fusion methods, such as multi-structure [79] and multi-stage model fusion [80], is another viable way to facilitate the model interpretation of battery internal dynamics, while remaining an acceptable model complexity. It is believed that the model fusion method is a promising alternative to achieve the improved performance in SOP estimation.

5.2. Parameter Identification Techniques

Online and offline parameter identification techniques have their own advantages and disadvantages for SOP estimation. On the one hand, online techniques achieve the optimal parameters estimation at the present moment by minimizing the errors between the estimated model outputs and measurements, which leads to preferable adaptability and robustness over offline techniques under complex operating conditions over battery lifetime [81,82]. On the other hand, online estimated model parameters attempt to track battery current–voltage characteristics, under changeable operating conditions, resulting in a small time constant of RC network. Nonetheless, a battery operating at the peak discharge or charge currents in a prediction window ranging from 10 s up to 120 s requires a relatively large time constant of RC networks to reflect its dynamics during this period. Therefore, online estimated model parameters, under a dynamic load profile, may not accurately capture the battery behaviour in SOP estimation. The longer the prediction window, the worse the model accuracy. Moreover, online techniques treat battery dynamics under excitation and during relaxation in a mutual time constant, while the research in [83] discovered that a battery will show a noticeably distinction in time constants between these two operations. The experimental results demonstrate a compromised performance in battery voltage prediction, using a mutual time constant.

By contrast, offline techniques are free of the aforementioned limitations in online techniques, which could separately capture model parameters, considering various factors, such as current direction and load conditions. In addition, they are able to capture the variation trend of model parameters over a battery operating range (e.g., SOC and temperature) [84,85]. Hence, an approach with the combined strengths of both online and offline parameter identification techniques is expected to be developed for SOP estimation in the future. For instance, the model parameters of ECM in [86] are partially adapted online through a data-driven method and partially extracted offline, which achieves the improved robustness over battery service life.

5.3. Battery Multi-State Co-Estimation

Most of the relevant research in the literature focuses on two-state joint estimation of lithium-ion batteries [87,88]. However, the multi-state estimation of at least three battery states has not been sufficiently investigated. As pointed out in [8], different battery states reflect a hierarchical correlation, where accurate SOP estimation relies on the basis of SOC, SOH, and SOT, all of which can directly influence the model parameters of a battery system from different spatial and temporal scales. Also, SOE is proved as a more effective constraint over SOC for SOP estimation, from an energy management perspective [21,65]. Hence, joint estimation of two battery states or multi-state estimation in a parallel structure, while ignoring the multi-physics coupling effect in-between, which can only yield relatively satisfactory results under limited operating conditions [89]. In light of this, it is essential to advance the state-of-the-art joint estimation techniques one step forward and comprehensively engage those battery states in a coupled multi-state estimation algorithm to achieve a full-featured BMS.

5.4. Machine Learning

ECM-based methods have become the mainstream technology for online SOP estimation, due to their advantages of ease of implementation and computationally efficiency. However, their performance in capturing battery nonlinearity is always limited by the imperfect model structure and time-variant model parameters. On the other hand, machine learning-based methods, such as support vector machine and artificial neural network, have showed a prominent strength in mimicking battery nonlinearity and been widely leveraged in SOC and SOH estimation [90–92]. Research in this area could be made by directly collecting the testing data (e.g., voltage, current, SOC, and temperature) from different user-designed charge/discharge profiles and then extracting the underlying features [93]. Thus, designing an online SOP estimation method by fusing ECM-based method and machine learning is a viable way to facilitate the estimation accuracy and achieve preferable performance. Nevertheless, as introduced in the previous section, SOP reference acquisition has been a very challenging task over a whole battery operating range in a variable prediction window, when the effects of temperature and battery aging are taken into account. As a result, it can be considerably time-consuming and laborious to collect high-quality data to train machine learning-based methods. An effective way to overcome the data scarcity of SOP references is data augmentation, where generative adversarial networks [94] and variational autoencoders [95] are two useful tools that have been recently employed in SOC estimation and the remaining useful life prediction for lithium-ion batteries. With more applications of data augmentation techniques, it can be expected that machine learning will have more applications in online SOP estimation and become a future research direction.

5.5. Validation Approach

Until now, there is no a standard or uniform validation approach for SOP estimation [74]. As a result, a question mark is hanging over the reliability of existing online SOP estimation techniques. Besides, most of the existing SOP testing methods have not taken dynamic driving conditions into account, and they only measure battery SOP from a fully established state, while neglecting the initial battery polarisation voltage at the beginning of a prediction window under dynamic load profiles. In this regard, a reliable and efficient SOP calibration method is expected to be devised to allow for performance comparison among different SOP estimation techniques.

6. Conclusions

In this paper, the improvements on ECM-based online SOP estimation methods in the past decade are reviewed. Basic principles of online SOP estimation are firstly introduced according to different operation modes. Afterwards, the research progress on ECM-based online SOP estimation methods is systematically overviewed from three perspectives: battery modelling, model parameters identification, and SOP estimation. Technical contributions are highlighted, and critical analysis is provided. Additionally, SOP testing methods are discussed for their accuracy and efficiency. Finally, challenges and outlooks of online SOP estimation are summarized, with an intention to spur relevant researchers to conceive of innovative ideas for further research developments.

Author Contributions: Conceptualization and writing—original draft preparation, R.G.; writing—review and editing, W.S. and R.G.; conceptualization and supervision, W.S. All authors have read and agreed to the published version of the manuscript.

Funding: This research is funded by the Australian government research training program scholarship, offered to the first author of this study.

Conflicts of Interest: The authors declare no conflict of interest.

Nomenclature

AFFLS	Adaptive forgetting factor least square
AFFRTLS	Adaptive forgetting factor recursive total least square
ANFIS	Adaptive neuro-fuzzy inference system
BMS	Battery management system
BVE	Butler–Volmer equation
CC	Constant current
CCCV	Constant current constant voltage
CM	Characteristic mapping
CP	Constant power
CV	Constant voltage
CVCP	Constant voltage constant power
DAEKF	Dual adaptive extended Kalman filter
DEKF	Dual extended Kalman filter
DMC	Dynamic matrix control
DP	Dual polarisation
ECM	Equivalent circuit model
EIS	Electrochemical impedance spectroscopy
EKF	Extended Kalman filter
ELM	Extreme learning machine
EV	Electrical vehicle
FFRLS	Forgetting factor recursive least square
GA	Genetic algorithm
HPPC	Hybrid pulse power characterization
KF	Kalman filter
MHE	Moving horizon estimation
MMPI	Multistep model predictive iterative
MPC	Model predictive control
OCV	Open-circuit voltage
OLPM	Open-loop prediction method
PSO	Particle swarm optimisation
RLS	Recursive least square
SOC	State of charge
SOE	State of energy
SOH	State of health
SOP	State of power
SOT	State of temperature
UKF	Unscented Kalman filter
VLERO	Voltage limited with extrapolation of resistances and open-circuit voltage
WRLS	Weighted recursive least square

References

- Tran, M.-K.; Akinsanya, M.; Panchal, S.; Fraser, R.; Fowler, M. Design of a Hybrid Electric Vehicle Powertrain for Performance Optimization Considering Various Powertrain Components and Configurations. *Vehicles* **2021**, *3*, 20–32. [[CrossRef](#)]
- Hu, X.; Zou, C.; Zhang, C.; Li, Y. Technological Developments in Batteries: A Survey of Principal Roles, Types, and Management Needs. *IEEE Power Energy Mag.* **2017**, *15*, 20–31. [[CrossRef](#)]
- Scrosati, B.; Garche, J. Lithium Batteries: Status, Prospects and Future. *J. Power Sources* **2010**, *12*, 2419–2430. [[CrossRef](#)]
- Varga, B.O. Electric Vehicles, Primary Energy Sources and CO₂ Emissions: Romanian Case Study. *Energy* **2013**, *49*, 61–70. [[CrossRef](#)]
- Han, W.; Altaf, F.; Zou, C.; Wik, T. State of Power Prediction for Battery Systems with Parallel-Connected Units. *IEEE Trans. Transp. Electrif.* **2021**, *1*. [[CrossRef](#)]
- Van Reeve, V.; Hofman, T. Multi-Level Energy Management for Hybrid Electric Vehicles—Part I. *Vehicles* **2019**, *1*, 3–40. [[CrossRef](#)]
- Van Reeve, V.; Hofman, T. Multi-Level Energy Management—Part II: Implementation and Validation. *Vehicles* **2019**, *1*, 41–56. [[CrossRef](#)]
- Hu, X.; Jiang, H.; Feng, F.; Liu, B. An Enhanced Multi-State Estimation Hierarchy for Advanced Lithium-Ion Battery Management. *Appl. Energy* **2020**, *257*, 114019. [[CrossRef](#)]

9. Farmann, A.; Sauer, D.U. A Comprehensive Review of On-Board State-of-Available-Power Prediction Techniques for Lithium-Ion Batteries in Electric Vehicles. *J. Power Sources* **2016**, *329*, 123–137. [[CrossRef](#)]
10. Plett, G.L. High-Performance Battery-Pack Power Estimation Using a Dynamic Cell Model. *IEEE Trans. Veh. Technol.* **2004**, *53*, 1586–1593. [[CrossRef](#)]
11. Sun, F.; Xiong, R.; He, H.; Li, W.; Aussems, J.E.E. Model-Based Dynamic Multi-Parameter Method for Peak Power Estimation of Lithium-Ion Batteries. *Appl. Energy* **2012**, *96*, 378–386. [[CrossRef](#)]
12. Sun, F.; Xiong, R.; He, H. Estimation of State-of-Charge and State-of-Power Capability of Lithium-Ion Battery Considering Varying Health Conditions. *J. Power Sources* **2014**, *259*, 166–176. [[CrossRef](#)]
13. Wang, S.; Verbrugge, M.; Wang, J.S.; Liu, P. Multi-Parameter Battery State Estimator Based on the Adaptive and Direct Solution of the Governing Differential Equations. *J. Power Sources* **2011**, *196*, 8735–8741. [[CrossRef](#)]
14. Pei, L.; Zhu, C.; Wang, T.; Lu, R.; Chan, C.C. Online Peak Power Prediction Based on a Parameter and State Estimator for Lithium-Ion Batteries in Electric Vehicles. *Energy* **2014**, *66*, 766–778. [[CrossRef](#)]
15. Zhang, H.; Chow, M.-Y. Comprehensive Dynamic Battery Modeling for PHEV Applications. In Proceedings of the IEEE PES General Meeting, IEEE, Minneapolis, MN, USA, 25–29 August 2010; pp. 1–6.
16. Hu, X.; Li, S.; Peng, H. A Comparative Study of Equivalent Circuit Models for Li-Ion Batteries. *J. Power Sources* **2012**, *198*, 359–367. [[CrossRef](#)]
17. Lai, X.; Zheng, Y.; Sun, T. A Comparative Study of Different Equivalent Circuit Models for Estimating State-of-Charge of Lithium-Ion Batteries. *Electrochim. Acta* **2018**, *259*, 566–577. [[CrossRef](#)]
18. Wang, X.; Wei, X.; Zhu, J.; Dai, H.; Zheng, Y.; Xu, X.; Chen, Q. A Review of Modeling, Acquisition, and Application of Lithium-Ion Battery Impedance for Onboard Battery Management. *eTransportation* **2021**, *7*, 100093. [[CrossRef](#)]
19. Wang, S.; Verbrugge, M.; Wang, J.S.; Liu, P. Power Prediction from a Battery State Estimator That Incorporates Diffusion Resistance. *J. Power Sources* **2012**, *214*, 399–406. [[CrossRef](#)]
20. Hu, X.; Xiong, R.; Egardt, B. Model-Based Dynamic Power Assessment of Lithium-Ion Batteries Considering Different Operating Conditions. *IEEE Trans. Ind. Inf.* **2014**, *10*, 1948–1959. [[CrossRef](#)]
21. Wang, Y.; Pan, R.; Liu, C.; Chen, Z.; Ling, Q. Power Capability Evaluation for Lithium Iron Phosphate Batteries Based on Multi-Parameter Constraints Estimation. *J. Power Sources* **2018**, *374*, 12–23. [[CrossRef](#)]
22. Wei, C.; Benosman, M. Extremum Seeking-Based Parameter Identification for State-of-Power Prediction of Lithium-Ion Batteries. In Proceedings of the 2016 IEEE International Conference on Renewable Energy Research and Applications (ICRERA), IEEE, Birmingham, UK, 20–23 November 2016; pp. 67–72.
23. Xiang, S.; Hu, G.; Huang, R.; Guo, F.; Zhou, P. Lithium-Ion Battery Online Rapid State-of-Power Estimation under Multiple Constraints. *Energies* **2018**, *11*, 283. [[CrossRef](#)]
24. Dong, G.; Wei, J.; Chen, Z. Kalman Filter for Onboard State of Charge Estimation and Peak Power Capability Analysis of Lithium-Ion Batteries. *J. Power Sources* **2016**, *328*, 615–626. [[CrossRef](#)]
25. Feng, T.; Yang, L.; Zhao, X.; Zhang, H.; Qiang, J. Online Identification of Lithium-Ion Battery Parameters Based on an Improved Equivalent-Circuit Model and Its Implementation on Battery State-of-Power Prediction. *J. Power Sources* **2015**, *281*, 192–203. [[CrossRef](#)]
26. Jiang, J.; Liu, S.; Ma, Z.; Wang, L.Y.; Wu, K. Butler-Volmer Equation-Based Model and Its Implementation on State of Power Prediction of High-Power Lithium Titanate Batteries Considering Temperature Effects. *Energy* **2016**, *117*, 58–72. [[CrossRef](#)]
27. Waag, W.; Fleischer, C.; Sauer, D.U. Adaptive On-Line Prediction of the Available Power of Lithium-Ion Batteries. *J. Power Sources* **2013**, *242*, 548–559. [[CrossRef](#)]
28. Tang, X.; Wang, Y.; Yao, K.; He, Z.; Gao, F. Model Migration Based Battery Power Capability Evaluation Considering Uncertainties of Temperature and Aging. *J. Power Sources* **2019**, *440*, 227141. [[CrossRef](#)]
29. Yang, L.; Cai, Y.; Yang, Y.; Deng, Z. Supervisory Long-Term Prediction of State of Available Power for Lithium-Ion Batteries in Electric Vehicles. *Appl. Energy* **2020**, *257*, 114006. [[CrossRef](#)]
30. Burgos-Mellado, C.; Orchard, M.E.; Kazerani, M.; Cárdenas, R.; Sáez, D. Particle-Filtering-Based Estimation of Maximum Available Power State in Lithium-Ion Batteries. *Appl. Energy* **2016**, *161*, 349–363. [[CrossRef](#)]
31. Zheng, F.; Jiang, J.; Sun, B.; Zhang, W.; Pecht, M. Temperature Dependent Power Capability Estimation of Lithium-Ion Batteries for Hybrid Electric Vehicles. *Energy* **2016**, *113*, 64–75. [[CrossRef](#)]
32. Zheng, L.; Zhu, J.; Wang, G.; Lu, D.D.-C.; McLean, P.; He, T. Experimental Analysis and Modeling of Temperature Dependence of Lithium-Ion Battery Direct Current Resistance for Power Capability Prediction. In Proceedings of the 2017 20th International Conference on Electrical Machines and Systems (ICEMS), IEEE, Sydney, Australia, 11–14 August 2017; pp. 1–4.
33. Wang, Y. Online Estimation of Battery Power State Based on Improved Equivalent Circuit Model. *IOP Conf. Ser. Earth Environ. Sci.* **2021**, *651*, 022080. [[CrossRef](#)]
34. Zou, C.; Klintberg, A.; Wei, Z.; Fridholm, B.; Wik, T.; Egardt, B. Power Capability Prediction for Lithium-Ion Batteries Using Economic Nonlinear Model Predictive Control. *J. Power Sources* **2018**, *396*, 580–589. [[CrossRef](#)]
35. Tan, Y.; Luo, M.; She, L.; Cui, X. Joint Estimation of Ternary Lithium-Ion Battery State of Charge and State of Power Based on Dual Polarization Model. *Int. J. Electrochem. Sci.* **2020**, *15*, 20. [[CrossRef](#)]
36. Shen, P.; Ouyang, M.; Lu, L.; Li, J.; Feng, X. The Co-Estimation of State of Charge, State of Health, and State of Function for Lithium-Ion Batteries in Electric Vehicles. *IEEE Trans. Veh. Technol.* **2017**, *67*, 92–103. [[CrossRef](#)]

37. Nejad, S.; Gladwin, D.T. Online Battery State of Power Prediction Using PRBS and Extended Kalman Filter. *IEEE Trans. Ind. Electron.* **2020**, *67*, 3747–3755. [[CrossRef](#)]
38. Niri, M.F.; Dinh, T.Q.; Yu, T.F.; Marco, J.; Bui, T.M.N. State of Power Prediction for Lithium-Ion Batteries in Electric Vehicles via Wavelet-Markov Load Analysis. *IEEE Trans. Intell. Transp. Syst.* **2020**, 1–16. [[CrossRef](#)]
39. Shu, X.; Li, G.; Shen, J.; Lei, Z.; Chen, Z.; Liu, Y. An Adaptive Multi-State Estimation Algorithm for Lithium-Ion Batteries Incorporating Temperature Compensation. *Energy* **2020**, *207*, 118262. [[CrossRef](#)]
40. Dubarry, M.; Liaw, B.Y. Development of a Universal Modeling Tool for Rechargeable Lithium Batteries. *J. Power Sources* **2007**, *174*, 856–860. [[CrossRef](#)]
41. Li, X.; Sun, J.; Hu, Z.; Lu, R.; Zhu, C.; Wu, G. A New Method of State of Peak Power Capability Prediction for Li-Ion Battery. In Proceedings of the 2015 IEEE Vehicle Power and Propulsion Conference (VPPC), IEEE, Montreal, QC, Canada, 19–22 October 2015; pp. 1–5.
42. Podlubny, I. *Fractional Differential Equations: An Introduction to Fractional Derivatives, Fractional Differential Equations, to Methods of Their Solution and Some of Their Applications*; Elsevier: Amsterdam, The Netherlands, 1998.
43. Liu, C.; Hu, M.; Jin, G.; Xu, Y.; Zhai, J. State of Power Estimation of Lithium-Ion Battery Based on Fractional-Order Equivalent Circuit Model. *J. Energy Storage* **2021**, *41*, 102954. [[CrossRef](#)]
44. Farmann, A.; Sauer, D.U. Comparative Study of Reduced Order Equivalent Circuit Models for On-Board State-of-Available-Power Prediction of Lithium-Ion Batteries in Electric Vehicles. *Appl. Energy* **2018**, *225*, 1102–1122. [[CrossRef](#)]
45. Lai, X. Co-Estimation of State of Charge and State of Power for Lithium-Ion Batteries Based on Fractional Variable-Order Model. *J. Clean. Prod.* **2020**, *255*, 120203. [[CrossRef](#)]
46. Gao, W.; Zou, Y.; Sun, F.; Hu, X.; Yu, Y.; Feng, S. Data Pieces-Based Parameter Identification for Lithium-Ion Battery. *J. Power Sources* **2016**, *328*, 174–184. [[CrossRef](#)]
47. Jiang, B.; Dai, H.; Wei, X.; Zhu, L.; Sun, Z. Online Reliable Peak Charge/Discharge Power Estimation of Series-Connected Lithium-Ion Battery Packs. *Energies* **2017**, *10*, 390. [[CrossRef](#)]
48. Xiong, R.; He, H.; Sun, F.; Liu, X.; Liu, Z. Model-Based State of Charge and Peak Power Capability Joint Estimation of Lithium-Ion Battery in Plug-in Hybrid Electric Vehicles. *J. Power Sources* **2013**, *229*, 159–169. [[CrossRef](#)]
49. Xiong, R.; He, H.; Sun, F.; Zhao, K. Online Estimation of Peak Power Capability of Li-Ion Batteries in Electric Vehicles by a Hardware-in-Loop Approach. *Energies* **2012**, *5*, 1455–1469. [[CrossRef](#)]
50. Xiong, R.; Sun, F.; Chen, Z.; He, H. A data-driven multi-scale extended Kalman filtering based parameter and state estimation approach of lithium-ion polymer battery in electric vehicles. *Appl. Energy* **2014**, *113*, 463–476. [[CrossRef](#)]
51. Li, B.; Wang, S.; Fernandez, C.; Yu, C.; Xia, L.; Fan, Y. A Linear Recursive State of Power Estimation Method Based on Fusion Model of Voltage and State of Charge Limitations. *J. Energy Storage* **2021**, *40*, 102583. [[CrossRef](#)]
52. Wei, Z.; Zhao, J.; Xiong, R.; Dong, G.; Pou, J.; Tseng, K.J. Online Estimation of Power Capacity With Noise Effect Attenuation for Lithium-Ion Battery. *IEEE Trans. Ind. Electron.* **2019**, *66*, 5724–5735. [[CrossRef](#)]
53. Plett, G.L. Dual and Joint EKF for Simultaneous SOC and SOH Estimation. In Proceedings of the 21st Electric Vehicle Symposium (EVS21), Monte Carlo, Monaco, 2–6 April 2005; pp. 1–12.
54. Juang, L.W.; Kollmeyer, P.J.; Jahns, T.M.; Lorenz, R.D. Implementation of Online Battery State-of-Power and State-of-Function Estimation in Electric Vehicle Applications. In Proceedings of the 2012 IEEE Energy Conversion Congress and Exposition (ECCE), IEEE, Raleigh, NC, USA, 15–20 September 2012; pp. 1819–1826.
55. Zhang, W.; Wang, L.; Wang, L.; Liao, C.; Zhang, Y. Joint State-of-Charge and State-of-Available-Power Estimation Based on the Online Parameter Identification of Lithium-Ion Battery Model. *IEEE Trans. Ind. Electron.* **2021**, *1*. [[CrossRef](#)]
56. Zhou, Z.; Kang, Y.; Shang, Y.; Cui, N.; Zhang, C.; Duan, B. Peak Power Prediction for Series-Connected LiNCM Battery Pack Based on Representative Cells. *J. Clean. Prod.* **2019**, *230*, 1061–1073. [[CrossRef](#)]
57. Waag, W.; Fleischer, C.; Sauer, D.U. On-Line Estimation of Lithium-Ion Battery Impedance Parameters Using a Novel Varied-Parameters Approach. *J. Power Sources* **2013**, *237*, 260–269. [[CrossRef](#)]
58. Zhang, X.; Wang, Y.; Wu, J.; Chen, Z. A Novel Method for Lithium-Ion Battery State of Energy and State of Power Estimation Based on Multi-Time-Scale Filter. *Appl. Energy* **2018**, *216*, 442–451. [[CrossRef](#)]
59. Chen, Z.; Lu, J.; Yang, Y.; Xiong, R. Online Estimation of State of Power for Lithium-Ion Battery Considering the Battery Aging. In Proceedings of the 2017 Chinese Automation Congress (CAC), IEEE, Jinan, China, 20–22 October 2017; pp. 3112–3116.
60. Lu, J.; Chen, Z.; Yang, Y.; Ming, L.V. Online Estimation of State of Power for Lithium-Ion Batteries in Electric Vehicles Using Genetic Algorithm. *IEEE Access* **2018**, *6*, 20868–20880. [[CrossRef](#)]
61. Malysz, P.; Ye, J.; Gu, R.; Yang, H.; Emadi, A. Battery State-of-Power Peak Current Calculation and Verification Using an Asymmetric Parameter Equivalent Circuit Model. *IEEE Trans. Veh. Technol.* **2016**, *65*, 11. [[CrossRef](#)]
62. Wang, L.; Cheng, Y.; Zou, J. Battery Available Power Prediction of Hybrid Electric Vehicle Based on Improved Dynamic Matrix Control Algorithms. *J. Power Sources* **2014**, *261*, 337–347. [[CrossRef](#)]
63. Esfandyari, M.J.; Hairi Yazdi, M.R.; Esfahanian, V.; Masih-Tehrani, M.; Nehzati, H.; Shekoofa, O. A Hybrid Model Predictive and Fuzzy Logic Based Control Method for State of Power Estimation of Series-Connected Lithium-Ion Batteries in HEVs. *J. Energy Storage* **2019**, *24*, 100758. [[CrossRef](#)]
64. Esfandyari, M.J.; Esfahanian, V.; Hairi Yazdi, M.R.; Nehzati, H.; Shekoofa, O. A New Approach to Consider the Influence of Aging State on Lithium-Ion Battery State of Power Estimation for Hybrid Electric Vehicle. *Energy* **2019**, *176*, 505–520. [[CrossRef](#)]

65. Zhang, W.; Shi, W.; Ma, Z. Adaptive Unscented Kalman Filter Based State of Energy and Power Capability Estimation Approach for Lithium-Ion Battery. *J. Power Sources* **2015**, *289*, 50–62. [[CrossRef](#)]
66. Zhang, T.; Guo, N.; Sun, X.; Fan, J.; Yang, N.; Song, J.; Zou, Y. A Systematic Framework for State of Charge, State of Health and State of Power Co-Estimation of Lithium-Ion Battery in Electric Vehicles. *Sustainability* **2021**, *13*, 5166. [[CrossRef](#)]
67. Rahimifard, S.; Ahmed, R.; Habibi, S. Interacting Multiple Model Strategy for Electric Vehicle Batteries State of Charge/Health/Power Estimation. *IEEE Access* **2021**, *9*, 109875–109888. [[CrossRef](#)]
68. Fleischer, C.; Waag, W.; Bai, Z.; Sauer, D.U. Self-Learning State-of-Available-Power Prediction for Lithium-Ion Batteries in Electrical Vehicles. In Proceedings of the 2012 IEEE Vehicle Power and Propulsion Conference, Seoul, South Korea, 9–12 October 2012; pp. 370–375.
69. Tang, X.; Yao, K.; Liu, B.; Hu, W.; Gao, F. Long-Term Battery Voltage, Power, and Surface Temperature Prediction Using a Model-Based Extreme Learning Machine. *Energies* **2018**, *11*, 86. [[CrossRef](#)]
70. Roşca, B.; Wilkins, S.; Jacob, J.; Hoedemaekers, E.; Van Den Hoek, S. Predictive Model Based Battery Constraints for Electric Motor Control within EV Powertrains. In Proceedings of the 2014 IEEE International Electric Vehicle Conference (IEVC), IEEE, Florence, Italy, 17–19 December 2014; pp. 1–8.
71. Li, X.; Xu, J.; Hong, J.; Tian, J.; Tian, Y. State of Energy Estimation for a Series-Connected Lithium-Ion Battery Pack Based on an Adaptive Weighted Strategy. *Energy* **2021**, *214*, 118858. [[CrossRef](#)]
72. Zhang, C.; Sharkh, S.M. Estimation of Real-Time Peak Power Capability of a Traction Battery Pack Used in an HEV. In Proceedings of the 2010 Asia-Pacific Power and Energy Engineering Conference, IEEE, Chengdu, China, 28–31 March 2010; pp. 1–6.
73. Shen, X.; Sun, B.; Qi, H.; Shen, X.; Su, X. Research on Peak Power Test Method for Lithium Ion Battery. *Energy Procedia* **2018**, *152*, 550–555. [[CrossRef](#)]
74. Jin, C.; Sun, Y.; Zheng, Y.; Yang, X.; Lai, X.; Gu, H.; Feng, X. Experimental Investigation of State-of-power Measurement for Lithium-ion Batteries. *Int. J. Energy Res.* **2021**, *45*, 7549–7560. [[CrossRef](#)]
75. Hunt, G.; Motloch, C. *Freedom Car Battery Test Manual for Power-Assist Hybrid Electric Vehicles*; INEEL: Falls, ID, USA, 2003; pp. 3–6.
76. Xiong, R.; Tian, J.; Shen, W.; Sun, F. A Novel Fractional Order Model for State of Charge Estimation in Lithium Ion Batteries. *IEEE Trans. Veh. Technol.* **2019**, *68*, 4130–4139. [[CrossRef](#)]
77. Tian, J.; Xiong, R.; Yu, Q. Fractional-Order Model-Based Incremental Capacity Analysis for Degradation State Recognition of Lithium-Ion Batteries. *IEEE Trans. Ind. Electron.* **2018**, *66*, 1576–1584. [[CrossRef](#)]
78. Ling, L.; Wei, Y. State-of-Charge and State-of-Health Estimation for Lithium-Ion Batteries Based on Dual Fractional-Order Extended Kalman Filter and Online Parameter Identification. *IEEE Access* **2021**, *9*, 47588–47602. [[CrossRef](#)]
79. Lin, C.; Mu, H.; Xiong, R.; Shen, W. A Novel Multi-Model Probability Battery State of Charge Estimation Approach for Electric Vehicles Using H-Infinity Algorithm. *Appl. Energy* **2016**, *166*, 76–83. [[CrossRef](#)]
80. Xiong, R.; Wang, J.; Shen, W.; Tian, J.; Mu, H. Co-Estimation of State of Charge and Capacity for Lithium-Ion Batteries with Multi-Stage Model Fusion Method. *Engineering* **2021**, S2095809921000163. [[CrossRef](#)]
81. Lao, Z.; Xia, B.; Wang, W.; Sun, W.; Lai, Y.; Wang, M. A Novel Method for Lithium-Ion Battery Online Parameter Identification Based on Variable Forgetting Factor Recursive Least Squares. *Energies* **2018**, *11*, 1358. [[CrossRef](#)]
82. Tan, X.; Zhan, D.; Lyu, P.; Rao, J.; Fan, Y. Online State-of-Health Estimation of Lithium-Ion Battery Based on Dynamic Parameter Identification at Multi Timescale and Support Vector Regression. *J. Power Sources* **2021**, *484*, 229233. [[CrossRef](#)]
83. Hua, X.; Zhang, C.; Offer, G. Finding a Better Fit for Lithium Ion Batteries: A Simple, Novel, Load Dependent, Modified Equivalent Circuit Model and Parameterization Method. *J. Power Sources* **2021**, *484*, 229117. [[CrossRef](#)]
84. Zhang, J.; Wang, P.; Liu, Y.; Cheng, Z. Variable-Order Equivalent Circuit Modeling and State of Charge Estimation of Lithium-Ion Battery Based on Elec-trochemical Impedance Spectroscopy. *Energies* **2021**, *14*, 769. [[CrossRef](#)]
85. Li, Z.; Shi, X.; Shi, M.; Wei, C.; Di, F.; Sun, H. Investigation on the Impact of the HPPC Profile on the Battery ECM Parameters' Offline Identification. In Proceedings of the 2020 Asia Energy and Electrical Engineering Symposium (AEEES), IEEE, Chengdu, China, 29–31 May 2020; pp. 753–757.
86. Song, Y.; Liu, D.; Liao, H.; Peng, Y. A Hybrid Statistical Data-Driven Method for on-Line Joint State Estimation of Lithium-Ion Batteries. *Appl. Energy* **2020**, *261*, 114408. [[CrossRef](#)]
87. Hu, X.; Yuan, H.; Zou, C.; Li, Z.; Zhang, L. Co-Estimation of State of Charge and State of Health for Lithium-Ion Batteries Based on Fractional-Order Calculus. *IEEE Trans. Veh. Technol.* **2018**, *67*, 10319–10329. [[CrossRef](#)]
88. Xiong, R.; Zhang, Y.; He, H.; Zhou, X.; Pecht, M.G. A Double-Scale, Particle-Filtering, Energy State Prediction Algorithm for Lithium-Ion Batteries. *IEEE Trans. Ind. Electron.* **2018**, *65*, 1526–1538. [[CrossRef](#)]
89. Hu, X.; Feng, F.; Liu, K.; Zhang, L.; Xie, J.; Liu, B. State Estimation for Advanced Battery Management: Key Challenges and Future Trends. *Renew. Sustain. Energy Rev.* **2019**, *114*, 109334. [[CrossRef](#)]
90. Lipu, M.H.; Hannan, M.; Hussain, A.; Saad, M.H.M.; Ayob, A.; Muttaqi, K.M. Lithium-Ion Battery State of Charge Estimation Method Using Optimized Deep Recurrent Neural Network Algorithm. In Proceedings of the 2019 IEEE Industry Applications Society Annual Meeting, IEEE, Baltimore, MD, USA, 29 September–3 October 2019; pp. 1–9.
91. Hannan, M.A.; Lipu, M.H.; Hussain, A.; Ker, P.J.; Mahlia, T.; Mansor, M.; Ayob, A.; Saad, M.H.; Dong, Z. Toward Enhanced State of Charge Estimation of Lithium-Ion Batteries Using Optimized Machine Learning Techniques. *Sci. Rep.* **2020**, *10*, 1–15.
92. Tian, J.; Xiong, R.; Shen, W.; Sun, F. Electrode Ageing Estimation and Open Circuit Voltage Reconstruction for Lithium Ion Batteries. *Energy Storage Mater.* **2021**, *37*, 283–295. [[CrossRef](#)]

93. Hannan, M.A.; Lipu, M.S.H.; Hussain, A.; Mohamed, A. A Review of Lithium-Ion Battery State of Charge Estimation and Management System in Electric Vehicle Applications: Challenges and Recommendations. *Renew. Sustain. Energy Rev.* **2017**, *78*, 834–854. [[CrossRef](#)]
94. Naaz, F.; Herle, A.; Channegowda, J.; Raj, A.; Lakshminarayanan, M. A Generative Adversarial Network-Based Synthetic Data Augmentation Technique for Battery Condition Evaluation. *Int. J. Energy Res.* **2021**, *45*, 19120–19135. [[CrossRef](#)]
95. Jiao, R.; Peng, K.; Dong, J. Remaining Useful Life Prediction of Lithium-Ion Batteries Based on Conditional Variational Autoencoders-Particle Filter. *IEEE Trans. Instrum. Meas.* **2020**, *69*, 8831–8843. [[CrossRef](#)]